J. Fluid Mech. (1992), *vol.* 241, *pp.* 261–289
Printed in Great Britain

The interaction between a high-frequency gust and a blade row

By N. PEAKE

Department of Applied Mathematics and Theoretical Physics, University of Cambridge, Silver Street, Cambridge CB3 9EW, UK

(Received 10 October 1991)

The ingestion of convected vorticity by a high-solidity rotating blade row is a potent noise source in modern aeroengines, due largely to the high level of mutual aerodynamic interactions between adjacent blades. In order to model this process we solve the problem of determining the unsteady lift on an infinite cascade of finite-chord flat plates due to an incident vorticity wave. The method of solution is the Wiener–Hopf technique, and we consider the case of the reduced frequency, Ω, being large, allowing application of asymptotic analysis in the formal limit $\Omega \to \infty$. This approach yields considerable simplification, both in allowing the truncation of an infinite reflection series to just two terms, and in allowing algebraic expressions for the Wiener–Hopf split functions to be found. The unsteady lift distribution is derived in closed form, and the accuracy of the asymptotic Wiener–Hopf factorization demonstrated for even modest values of Ω by comparison with exact (but less tractable) methods. Our formulae can easily be incorporated into existing noise prediction codes; the advantage of our scheme is that it handles a regime in which conventional numerical approaches become unwieldy, as well as providing significant physical insight into the underlying mechanisms.

1. Introduction

A clear understanding of the complicated unsteady flow processes in rotating turbo-machinery is of fundamental importance in the design of advanced aeroengines, and an issue of much concern in this respect is the question of sound generation by such systems, particularly in view of the stringency of mandatory noise certification levels around many of the world's busiest airports. Given the development and commissioning costs involved in engine manufacture, theoretical methods of predicting the noise are required; direct numerical computation of the far-field radiation using CFD-type codes is generally unsatisfactory, however, and progress must be made using semi-analytical schemes, and by solving model problems. In this direction considerable effort has already gone into developing noise prediction schemes for advanced propeller and propfan configurations, but much of this work cannot be applied directly to more conventional aeroengines or to the prototype ducted contra-fans currently under consideration as future powerplants for passenger aircraft, because blade aerodynamic interactions are neglected in the propeller analysis (this is certainly a good approximation for modern propellers, with typically 7 or 8 blades, but breaks down for the ducted systems where the blade count might be as high as 50). The aim of this paper is to describe an analytical prescription for extending existing propeller noise prediction schemes to the prediction of the sound generated by systems with closely spaced blades.

The blade aerodynamic interactions, or *cascade effects*, arise in a number of different ways; for instance, the merging of wakes shed by adjacent elements in a blade row, or changes in the isolated-blade potential field due to the proximity of nearest neighbours. However, the specific case we consider in this paper, and the one which is thought to be of particular importance in practice, is the question of *blade row response*. We have in mind the question of the sound produced when vorticity generated by some upstream obstruction (e.g. the wake shed by an inlet guide vane) interacts with a rotating blade row (e.g. the fan). The cascade effects here will include the multiple reflections of sound within the blade row, and the rescattering by leading and trailing edges; these effects would not be included in conventional propeller analysis, such as Parry & Crighton's (1989) contra-rotating propeller noise prediction scheme. The method we shall adopt will be a variant of Lighthill's (1952, 1954) acoustic analogy. Lighthill's theory, as originally formulated, states that the sound generated by a turbulent jet is exactly equal to that produced by an equivalent, fictitious distribution of quadrupoles. We emphasize that there will be no quadrupole distribution present in our problem to leading order, since we will suppose that the blades are thin and apply linear theory; however, Lighthill's approach can still be adopted in our linearized cascade analysis, and now states that the radiation generated by the rotating blades is equal to that produced by the equivalent distribution of (in this case) *force dipoles*. Therefore, provided that the unsteady lift distribution on the blades due to the interaction can be estimated by some analytical or numerical means, this acoustic analogy gives us an integral prescription for determining the radiation at infinity, by application of standard radiation integrals. Indeed, such integrals have already been found for rotating systems (see Parry & Crighton 1989); what remains to be calculated here is the unsteady life distribution on the blades.

In order to model the cascade process mathematically, and to produce a practical prediction scheme, some simplifications are required. The incident (helical) wake structure will be decomposed into its Fourier modes (again, see Parry & Crighton 1989 for details); we shall consider just a single harmonic gust, and here neglect the component of the upwash velocity parallel to the downstream blade row as being insignificant in the noise generation. We emphasize that the analysis in this paper could be repeated, with little modification, for incident *sound* waves, and would then be of particular interest in predicting levels of 'rotor blockage' (i.e. the degree to which engine noise is attenuated in passing through a blade row); we restrict attention here, however, to the case of incident *vorticity* waves. Effects of blade thickness and camber will also be neglected, and the blades modelled as parallel, thin plates (a computer-intensive method for inclusion of camber and thickness has been described by Verdon & Hall 1990). The blade row is 'unwrapped' into an infinite linear cascade, so that the flow at one particular radial station is mapped onto a two-dimensional plane; this is of course invalid if significant radial velocities exist, or if the radius in question is too close to the hub (so that the local curvature is too great), but will be acceptable as a first approximation along much of the blade. However, it is clear that the unwrapped geometry will not provide a sensible representation of the full three-dimensional problem at large distances from the blade row; after all, the actual motion of each blade element is along an advance helix, whilst in our two-dimensional approximation the blades move in straight lines. The two-dimensional version will not be able to provide sensible estimates of the full, three-dimensional radiation field at infinity; it will, however, give reliable predictions of those

quantities which are insensitive to long-range, three-dimensional effects, and, in particular, of the lift distribution on the blade surfaces.

The level of cascade effects in our model will depend on two important parameters. First, the *solidity*, defined to be the ratio of blade chord, c, to blade spacing, s; in the low-solidity propeller case, cascade effects will be small, but will become increasingly important as the inter-blade separation is decreased. No restriction on the value of the solidity will be necessary in our analysis, nor on the space–chord ratio (i.e. the separation between adjacent leading edges divided by the blade chord), with the one proviso that adjacent blades must overlap. Our model will therefore certainly be applicable to modern turbomachinery systems, in which the solidity and space–chord ratio are typically order unity. Second, the *reduced frequency*, Ω, defined by

$$\Omega = \omega c/U,$$

where ω is the gust frequency and U is the uniform free-stream velocity; in the ultra-high Ω limit, each blade would act as an isolated, semi-infinite plate, and cascade effects would be negligible. However, for more moderate values of Ω they certainly will be significant, especially if the gust wavelength is comparable to the blade spacing. Moderately large Ω values will be considered here (typically in the range $10 < \Omega < 20$); such values certainly occur in practical situations, but as will be seen later, are difficult to handle using existing computational techniques. It should also be noted that for high, subsonic mean flow the analysis described in this paper might also be required, even if Ω is small; in the co-moving frame the gust frequency will be $\omega/(1-M^2)^{\frac{1}{2}}$, so for Mach numbers, M, close to unity the effective reduced frequency could well be within our range of interest. In this paper we shall primarily be concerned with the effect of varying Ω, and in the numerical examples given the solidity will be held fixed.

A considerable body of literature already exists on this problem, typically involving solution by use of the Wiener–Hopf technique. Some of the earliest work was completed by Carlson & Heins (1946), Heins & Carlson (1947) and Heins (1950) who considered the related problem of electromagnetic waves incident on a cascade of semi-infinite conducting plates, and were able to evaluate transmission and reflection coefficients for the scattered radiation. A more complete description of both the Dirichlet and Von Neumann problems in this geometry is given by Meister (1962*a*, *b*). Mani & Horvay (1970) consider sound waves incident on a cascade of finite rigid plates, and approximate the effect of the trailing edges of the cascade by inclusion of the first two terms in an infinite reflection series. A more complete solution, including the full reflection series, is given by Koch (1971, 1983); both Mani & Horvay and Koch found only the amplitudes of the reflected and transmitted waves (representing the radiation at infinity), although the usefulness of such quantities in the two-dimensional problem is questionable, as discussed above. Of fundamental importance is the factorization of the Wiener–Hopf kernel function, and in each of the works cited above this is achieved via infinite product decomposition. The factors in these infinite products represent modes radiated in directions ahead of and behind the cascade, and duct modes between the blades. There are, of course, an infinity of such modes, but only a finite number of them possess real wavenumbers (i.e. are cut on). In order to make an accurate prediction of the radiation in the two-dimensional problem, all these propagating modes must be considered, together with the first few cut-off modes (Koch includes the first two cut-off modes in his analysis). In addition, we note that the amplitude of the radiation depends on the modulus (and not the phase) of each Wiener–Hopf factor,

and that these moduli only depend on the cut-on modes. At low frequency the number of such cut-on modes is small (indeed, in the case considered by Koch, there is just one propagating, plane-wave, duct mode), and therefore the approaches of Mani & Horvay and Koch are particularly numerically efficient in this regime, but require larger amounts of computer resource at high frequency (i.e. when more modes are cut on). Koch's method also suffers, at high frequency, from the need to invert a large matrix, essentially in determining the magnitudes of left- and right-propagating duct modes, which can be equally time-consuming.

When the pressure jump across the plates is required, however, Koch's infinite product factorization method cannot be used in practice for any frequency, both because of the complexity of the algebra, and because a large number of cut-off modes need to be included in order to find both the modulus and the phase of the pressure jump and in resolving the leading-edge singularity. As has already been argued, knowledge of the (two-dimensional) radiation at infinity is of limited practical use; the important quantity which can be extracted from the two-dimensional problem is the lift distribution, and to do this an alternative to Koch's method is required. Numerical techniques for calculating the pressure jump already exist (see in particular Kaji & Okazaki 1970*a*, *b*; Goldstein 1976; and the code LINSUB developed by Whitehead 1970), and work well for moderate reduced frequencies. Problems might arise for large Ω, however, because the number of grid points required to resolve the gust wavelength becomes large. Moreover, numerical schemes cannot provide the same level of physical insight as the kind of purely analytical solution presented here.

In this paper we describe a different approach to the problem of determining the lift distribution on the blades. The essential simplification (first suggested by Cargill 1988) is to consider only large reduced frequencies (i.e. the case for which existing numerical schemes become impractical), and apply asymptotic analysis in the limit $\Omega \to \infty$. The Wiener–Hopf kernel can now be factorized asymptotically, yielding closed algebraic expressions (retaining both modulus and phase). In addition, at high frequency, just the first two terms in the reflection series need be included (in parallel to Mani & Horvay's work), avoiding the need for large-matrix inversion. In §2 the mathematical formulation of the problem is described; in §3 the first term in the reflection series, corresponding to scattering of the incident gust by the blade leading edges, is found; whilst in §4 the second term, corresponding to the reflection of this first term by the trailing edges, is calculated. Inclusion of this second term allows our solution to satisfy the trailing-edge Kutta condition. The factorization of the split function is described in §5 (with mathematical details in Appendix A), involving the asymptotic evaluation of three distinct integrals via standard theory, and inclusion of both saddle point (scattered field) and pole (geometrical optics) contributions. Results are presented in §6 for a typical set of parameter values, and their accuracy assessed by comparison with the exact values found from the infinite-product theory (which is described in Appendix B for completeness).

The work described in this paper provides a relatively simple, fully analytical prescription for calculating the lift distribution on a cascade, at high reduced frequency; this information can then be used as input into existing acoustic prediction codes, to provide quick and accurate fan noise estimates. The advantage of our approach is that it can handle precisely those regimes in which numerical techniques become unwieldy, and an optimal strategy might well be to use a numerical scheme for moderate Ω, together with the asymptotic method in the high-frequency cases.

2. Mathematical formulation

We consider an infinite two-dimensional cascade, consisting of identical rigid thin blades; each blade is aligned parallel to the uniform subsonic mean flow, which has speed U and corresponding free-stream Mach number M. All physical variables are non-dimensionalized; lengths by the blade chord c; time by c/U; velocities by U; density perturbations by the undisturbed fluid density ρ_0; and pressure fluctuations by $\rho_0 U^2$. The blade spacing s, stagger d and stagger angle α and the coordinate axes are shown in figure 1. The blades are labelled $0, \pm 1, \pm 2, \ldots$, and we suppose that they overlap, (i.e. $d < 1$). A convected harmonic gust (corresponding to a transverse perturbation to the mean flow) is incident on the cascade from $x = -\infty$, so that the upwash normal to the nth blade is of the form

$$V_g \exp(\mathrm{i}\Omega t - \mathrm{i}\Omega x + \mathrm{i}n\sigma), \tag{1}$$

where V_g will be referred to as the *gust velocity*. The quantity σ, the *inter-blade phase angle*, represents the gust phase difference between adjacent blades and will depend in part on the upstream mechanism generating the disturbance (for instance, if the gust is a component of the periodic wake shed by a forward stator, σ would depend on the number of such stators, and on their rotational frequency measured in a frame in which the downstream row is fixed). Our choice of dimensionless variables means that s^{-1} is the solidity, and that the gust frequency is precisely the reduced frequency Ω. In the first instance we suppose that Ω has a small negative imaginary part, Ω_1, which will be set to zero at the end of the calculation.

The transverse gust velocity V_g will be taken as small, and the free-stream Mach number will be supposed to be not too close to unity; in the case the magnitude of the scattered field will also be small, and can be legitimately modelled using linear theory. According to Goldstein's (1976) splitting theorem, the perturbation velocity field can be decomposed into two components – the vortical part comprising the incident gust, and the irrotational scattered field – which are uncoupled under linear theory, and the scattered potential is therefore of the form $\varphi(x, y)\exp(\mathrm{i}\Omega t)$, with φ satisfying the time-reduced convected wave equation

$$\beta^2 \frac{\partial^2 \varphi}{\partial x^2} + \frac{\partial^2 \varphi}{\partial y^2} - 2\mathrm{i}M^2\Omega \frac{\partial \varphi}{\partial x} + M^2\Omega^2\varphi = 0, \tag{2}$$

where $\beta = (1 - M^2)^{\frac{1}{2}}$. The boundary conditions are

(i) the total normal velocity should vanish on the blades, i.e.

$$\frac{\partial \varphi}{\partial y} + V_g \exp(\mathrm{i}n\sigma - \mathrm{i}\Omega x) = 0 \tag{3}$$

on $\{0 \leqslant x \leqslant 1, y = ns\}$, for $n = 0, \pm 1, \pm 2, \ldots$;

(ii) the pressure, given by

$$p = -\left(\mathrm{i}\Omega + \frac{\partial}{\partial x}\right)\varphi, \tag{4}$$

is discontinuous across the blades, but is continuous everywhere else;

(iii) the scattered field must satisfy a radiation condition, which, with our introduction of the fictitious damping Ω_1, is equivalent to requiring φ to be bounded at infinity;

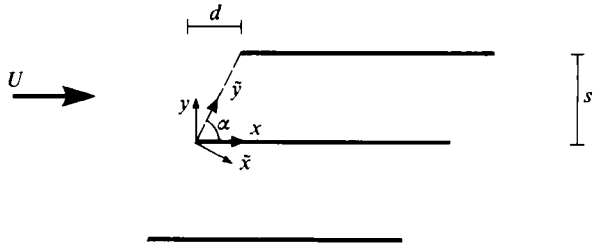

FIGURE 1. The blade system and coordinate axes.

(iv) finally, since the incident gust possesses the periodicity specified in (1), we shall further require that φ is also periodic with φ_n, the velocity potential in the strip $\{-\infty < x < \infty, ns \leqslant y \leqslant (n+1)s\}$, given by

$$\varphi_n(x,y) = \varphi_0(x-nd, y-ns)\exp(in\sigma); \tag{5}$$

the advantage of this approach is that only φ_0 need be calculated by applying the boundary conditions on just the zeroth blade, and the solution elsewhere determined from (5).

A method for solving this problem is described by Koch (1971), using the Wiener–Hopf technique. However, as previously noted, the complexity of this exact formulation is too great to allow the detailed phase information required in calculating the blade lift to be extracted; some simplification if therefore required, and will be made in this paper by supposing that the reduced frequency, Ω, is large. We begin from a different standpoint to that taken by Koch, and apply Schwarzchild's (1901) method (see also Landahl 1989), which provides a prescription for generating approximate solutions to three-part boundary-value problems. The scattered field in the zeroth strip, φ_0, is written in the form

$$\varphi_0 = \sum_{m=1}^{\infty} \phi_0^{(m)} + \sum_{m=1}^{\infty} \psi_0^{(m)}, \tag{6}$$

and the quantities $\phi_0^{(m)}$ and $\psi_0^{(m)}$ found by iterative solution of an infinite sequence of coupled, semi-infinite Wiener–Hopf problems. It is emphasized that (6) represents the exact solution to the problem, and that approximations are made by truncating the two power series to a finite number of terms. First, $\phi_0^{(1)}$ is calculated to satisfy the boundary conditions of zero total normal velocity on $\{x \geqslant 0, y = 0\}$ and zero pressure jump across $\{x < 0, y = 0\}$; this will include an error in the zero-pressure-jump boundary condition across $\{x \geqslant 1, y = 0\}$, so $\psi_0^{(1)}$ (with zero normal velocity on $\{x \leqslant 1, y = 0\}$ and a pressure jump across $\{x > 1, y = 0\}$ set to exactly cancel that due to $\phi_0^{(1)}$) is then found, to give an improved approximation $\phi_0^{(1)} + \psi_0^{(1)}$. However, $\psi_0^{(1)}$ will have a non-zero pressure jump across $\{x < 0, y = 0\}$, so a further term $\phi_0^{(2)}$ to balance this must be included, and so on. By induction, given that the first $N\phi_0^{(m)}$ terms and the first $(N-1)\psi_0^{(m)}$ terms have been calculated, $\psi_0^{(N)}$ is found to cancel the pressure jump of $\phi_0^{(N)}$ across $\{x > 1, y = 0\}$, and $\phi_0^{(N+1)}$ to cancel the pressure jump of $\psi_0^{(N)}$ across $\{x < 0, y = 0\}$. The inductive process is repeated until the desired accuracy is achieved; at each stage the pressure jump off the plates departs from its correct zero value by a small amount (dependent on the number of iterations already made). In the case of supersonic mean flow, $\phi_0^{(1)} + \psi_0^{(1)}$ is the exact solution to the problem (due to the absence of any trailing-edge influence upstream) – see Adamczyk & Goldstein

(1978) – but no such simplification is possible in our subsonic problem, and $\phi_0^{(m)}$ and $\psi_0^{(m)}$ are non-zero for all m.

Equation (6) can be interpreted as an infinite series of mode reflections by the leading and trailing edges. The incident gust will be scattered by the leading edge of the cascade, producing radiation in directions ahead of the blades, and possibly exciting cut-on modes (travelling in the positive x-direction) in the ducts between adjacent blades. If such propagating modes are produced (a plane-wave mode is always excited, but the existence of higher-order modes depends on Ω being sufficiently large), then they will subsequently be scattered by the trailing edges of the cascade, producing radiation in directions behind the blades, and inducing cut-on reflected duct modes. These left-travelling modes will in turn interact with the leading edges, generating an additional scattered field ahead of the blades, and further right-travelling modes in the blade passage, and the whole process repeats indefinitely. The terms in (6) can now be identified with these infinite reflections; the $\phi_0^{(m)}$ correspond to those modes which have been generated by the mth interaction with the leading edge, whilst $\psi_0^{(m)}$ correspond to those generated by the mth interaction with the trailing edges.

In the high-reduced-frequency limit, the reflection coefficients at the trailing edge will be small, essentially because the short-wavelength duct modes will pass through the open end of the duct virtually unhindered. We will therefore calculate just the first two terms in (6), in the formal limit $\Omega \to \infty$; in §3 the first term $\phi_0^{(1)}$ is calculated by considering the scattering of the incident gust by the leading edges of semi-infinite blades; in §4 the second term $\psi_0^{(1)}$ is found by solving the problem of the field $\phi_0^{(1)}$ incident on the trailing edges. Of course, more terms in the reflection series (6) could be included (as described above), but just the first two will be sufficient for large Ω (particularly in the light of the good results obtained by Mani & Horvay (1970), whose *ad hoc* approximation of including just one reflection is justified by our asymptotic analysis). A further step in completing our solution is the factorization of the Wiener–Hopf kernel function in §5 (and Appendix A), and our the high-frequency approach will yield considerably more physical insight than standard infinite-product methods, as well as providing greater computational efficiency with little loss in accuracy.

3. The leading-edge problem

In this section we shall calculate the $\phi_0^{(1)}$ term in (6) by considering the scattering of the incident gust (1) by an infinite cascade of *half-planes* $\{x > nd, y = ns; n = 0, \pm 1, \pm 2, \dots\}$, and as noted above we need only consider the strip between $y = 0$ and $y = s$. For convenience, we drop the superfix (1) when referring to $\phi_0^{(1)}$.

The Fourier transform is defined by

$$\Phi_0(k, y) = \int_{-\infty}^{\infty} \phi_0(x, y) \exp(\mathrm{i}kx)\, \mathrm{d}x, \tag{7}$$

and transforming (2) yields

$$\frac{\partial^2 \Phi_0}{\partial y^2} + \gamma^2 \Phi_0 = 0, \tag{8}$$

with

$$\gamma^2 = [M\Omega - k(1+M)]\,[M\Omega + k(1-M)]; \tag{9}$$

the branch cuts in the complex k-plane are shown in figure 2, and we suppose that

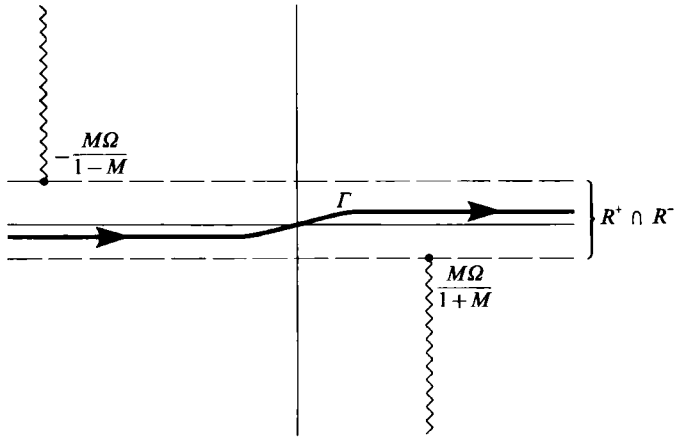

FIGURE 2. The complex k-plane.

γ takes negative imaginary values as $k \to +\infty$ along the real axis. Further, from (5) we have

$$\Phi_n(k, y) = \exp(in\sigma + inkd)\,\Phi_0(k, y - ns). \tag{10}$$

Equation (8) can be solved easily, and together with (10) implies that

$$\begin{aligned} \Phi_0(k, y) &= A\exp(-i\gamma y) + B\exp(i\gamma y), \\ \Phi_{-1}(k, y) &= \exp(-i\sigma - ikd)\{A\exp[-i\gamma(y+s)] + B\exp[i\gamma(y+s)]\}; \end{aligned} \tag{11}$$

since the normal velocity of the scattered field must be continuous across $Y = 0$ for all x, (11) implies that

$$A[1 - \exp(-i\sigma - ikd - i\gamma s)] = B[1 - \exp(-i\sigma - ikd + i\gamma s)]. \tag{12}$$

By taking the half-range Fourier transform (i.e. integrating over the interval $0 \leqslant x < \infty$) of the zero normal velocity boundary condition (equation (3)) we also have that

$$\frac{\partial \Phi_0^+}{\partial y}(k, 0) + \frac{iV_g}{k - \Omega} = 0, \tag{13}$$

where $\Phi_0^+(k, y)$ is simply the transform of $\phi_0(x, y)\,\mathrm{H}(x)$, and $\mathrm{H}(x)$ is the Heaviside step function. By transforming (4) we now write down an expression for the Fourier transform of the pressure jump across the zeroth blade, denoted by $[P_0^1(k, 0)]_-^+$ (with the superfix 1 indicating that this is the pressure jump associated with ϕ_0, i.e. with the leading-edge scattering), in terms of $\Phi_0(k, 0)$ and $\Phi_{-1}(k, 0)$; from (11), (12) and (13) we find, after some manipulation, that

$$\frac{[P_0^1(k, 0)]_-^+}{\mathscr{K}(k)} - \frac{\partial \Phi_0^-}{\partial y}(k, 0) + \frac{iV_g}{k - \Omega} = 0, \tag{14}$$

where $\Phi_0^-(k, y)$ is the transform of $\phi_0(x, y)\,\mathrm{H}(-x)$ and

$$\mathscr{K}(k) = \frac{\Omega - k}{\gamma}\left\{\frac{[\exp(-i\sigma - ikd + i\gamma s) - 1][1 - \exp(-i\sigma - ikd - i\gamma s)]}{i\sin(\gamma s)\exp(-i\sigma - ikd)}\right\}. \tag{15}$$

Equation (14) is a typical Wiener–Hopf equation with kernel $\mathscr{K}(k)$; the form of $\mathscr{K}(k)$ is very similar to that found by Koch (1971) and by Mani & Horvay (1970), and we note here that it is single-valued in the complex k-plane (because the direct dependence of (15) on γ is an even function), so that there will be no branch-cut contributions to subsequent integrals.

The k-plane is split into overlapping upper and lower half-planes R^+ and R^- respectively, defined by

$$\left\{k\in R^+ \,|\, \mathrm{Im}\,(k) > \frac{M\Omega_1}{1+M}\right\} \quad \text{and} \quad \left\{k\in R^- \,|\, \mathrm{Im}\,(k) < -\frac{M\Omega_1}{1-M}\right\},$$

and the kernel $\mathscr{K}(k)$ factorized as $\mathscr{K} = \mathscr{K}^+\mathscr{K}^-$, such that $\mathscr{K}^\pm(k)$ are analytic, non-zero and possess algebraic behaviour at infinity in $R^\pm$ respectively. The asymptotic evaluation of $\mathscr{K}^\pm(k)$ is described in §5. Since the pressure jump across $y = 0$ must be zero for $x < 0$, we note that $[P_0^1(\mathrm{k},0)]_-^+$ is analytic in R^+, and write (14) in the form

$$\begin{aligned} E(k) &= \frac{[P_0^1(k,0)]_-^+}{\mathscr{K}^+(k)} + \frac{\mathrm{i}V_g\,\mathscr{K}^-(\Omega)}{k-\Omega} \\ &= \mathscr{K}^-(k)\frac{\partial \Phi_0^-}{\partial y}(k,0) - \frac{\mathrm{i}V_g}{k-\Omega}(\mathscr{K}^-(k)-\mathscr{K}^-(\Omega)). \end{aligned} \tag{16}$$

The expressions on the right-hand side of (16) are analytic in R^+ and R^- respectively, and it therefore follows that $E(k)$ is analytic in both R^+ and R^-, and by analytic continuation in the whole complex plane; the facts that

$$\frac{\partial \phi_0}{\partial y}(x,0) \sim (-x)^{-\frac{1}{2}}$$

as $x \to -0$ and the pressure jump

$$[P_0^1(x,0)]_-^+ \sim x^{-\frac{1}{2}}$$

as $x \to +0$ (consequences of the flow being effectively incompressible, and therefore satisfying Laplace's equation, very near the leading edge), together with Liouville's theorem, lead to $E(k) \equiv 0$. Equation (16) therefore yields two equations, and it can finally be shown that

$$\Phi_0(k,y) = \frac{V_g\,\mathscr{K}^+(k)\,\mathscr{K}^-(\Omega)}{2(k-\Omega)^2}\left\{\frac{\exp(\mathrm{i}\sigma+\mathrm{i}kd)\cos(\gamma y)-\cos[\gamma(y-s)]}{\cos(\gamma s)-\cos(\sigma+kd)}\right\}; \tag{17}$$

or, in an alternative form,

$$\Phi_0(k,y) = \frac{V_g\,\mathscr{K}^-(\Omega)\exp(\mathrm{i}\sigma+\mathrm{i}kd)}{\mathrm{i}(k-\Omega)\gamma\mathscr{K}^-(k)\sin(\gamma s)}\{\cos[\gamma(y-s)]\exp(-\mathrm{i}\sigma-\mathrm{i}kd)-\cos(\gamma y)\}. \tag{18}$$

The scattered field will be recovered by inverting these Fourier transforms, and will consist of contributions from the relevant poles of $\Phi_0(k,y)$, and at this point we consider the location of all such poles. First, the denominator of (17) will certainly vanish for $k = \sigma_n$ satisfying

$$\pm\gamma s + (\sigma+kd) = 2n\pi \quad \text{for} \quad n = \ldots,-2,-1,0,1,2\ldots; \tag{19}$$

the σ_n will lie in both the upper half-plane (denoted σ_n^+) and in the lower half-plane (denoted σ_n^-), and can be found in the form

$$\sigma_n^{\pm} = \frac{d(2n\pi-\sigma)-M^2\Omega s^2 \mp [s^2(d^2+s^2)M^2\Omega^2 - 2dM^2\Omega s^2(2n\pi-\sigma)-s^2\beta^2(2n\pi-\sigma)^2]^{\frac{1}{2}}}{d^2+s^2\beta^2}, \tag{20}$$

for $-r \leqslant n \leqslant q$;

$$\sigma_n^{\pm} = \frac{d(2n\pi-\sigma)-M^2\Omega s^2 \pm \mathrm{i}[-s^2(d^2+s^2)M^2\Omega^2 + 2dM^2\Omega s^2(2n\pi-\sigma)+s^2\beta^2(2n\pi-\sigma)^2]^{\frac{1}{2}}}{d^2+s^2\beta^2}, \tag{21}$$

for $q < n < -r$, where q and $-r$ are the largest and smallest integers such that

$$s^2(d^2+s^2)M^2\Omega^2 - 2dM^2\Omega s^2(2n\pi-\sigma)-s^2\beta^2(2n\pi-\sigma)^2 \geqslant 0. \tag{22}$$

These $\sigma_n^{\pm}$ will be seen to correspond to modes radiated ahead of (and behind) the cascade. Second, the denominator of (18) will vanish for those $k = k_n^{\pm}$ (lying in the upper and lower half-planes respectively), satisfying

$$\gamma s = n\pi \quad \text{for} \quad n = 0, 1, 2, \ldots, \tag{23}$$

with

$$k_n^{\pm} = \begin{cases} \dfrac{-M^2\Omega \mp \left(M^2\Omega^2 - \beta^2\dfrac{n^2\pi^2}{s^2}\right)^{\frac{1}{2}}}{\beta^2} & \text{for} \quad n = 0, 1, \ldots, p; \qquad (24a) \\[2ex] \dfrac{-M^2\Omega \pm \mathrm{i}\left(\beta^2\dfrac{n^2\pi^2}{s^2} - M^2\Omega^2\right)^{\frac{1}{2}}}{\beta^2} & \text{for} \quad n = p+1, \ldots, \qquad (24b) \end{cases}$$

where p is the largest integer such that $(\beta^2\pi^2p^2/s^2) > M^2\Omega^2$. The $k_n^{\pm}$ correspond to the duct modes supported in the region of overlap between adjacent blades. We can check that these expressions for $\sigma_n^{\pm}$ and $k_n^{\pm}$ do indeed lie in the correct half-planes; this is clear in (21) and (24b), and is confirmed in (20) and (24a) by supposing Ω to be large, and defining the square root to take its principal value.

The scattered field is given by

$$\phi_0(x,y) = \frac{1}{2\pi}\int_{\Gamma} \Phi_0(k,y)\exp(-\mathrm{i}kx)\,\mathrm{d}k, \tag{25}$$

with the inversion contour Γ shown in figure 2. For $x<0$ we close Γ in the upper half-plane; from (17) the contributions to this integral will come purely from the poles at $k = \sigma_n^+$ (since $\mathscr{K}^+(k)$ is analytic in the upper half-plane, and $k = \Omega$ lies in the lower half-plane), but since this part of the solution is of no relevance to our main concern of the pressure jump across the blades, and since it is covered in detail by the authors previously cited, we will not give explicit expressions for the radiated field in $x<0$ here. However, for completeness we will demonstrate that our solution satisfies boundary condition (iii) (the radiation condition) (see §2), and to facilitate this we write (17) in the alternative form

$$\Phi_0(k,y) = \frac{V_g\mathscr{K}^+(k)\mathscr{K}^-(\Omega)}{2(k-\Omega)^2}\exp(\mathrm{i}\sigma+\mathrm{i}kd) \times\left\{\frac{\exp[\mathrm{i}\gamma(y-s)]}{1-\exp(-\mathrm{i}\gamma s+\mathrm{i}\sigma+\mathrm{i}kd)} - \frac{\exp[-\mathrm{i}\gamma(y-s)]}{1-\exp(\mathrm{i}\gamma s+\mathrm{i}\sigma+\mathrm{i}kd)}\right\}. \tag{26}$$

The value of $\gamma(\sigma_n^+)$ is uniquely determine for each pole σ_n^+ by our choice of branch cuts (equation (9) ff), and for each σ_n^+ just one of $\pm\gamma(\sigma_n^+)s+\sigma+\sigma_n^+ d = 2n\pi$ is satisfied. We suppose in the first instance that for a given σ_n^+ we have $+\gamma(\sigma_n^+)s+\sigma+\sigma_n^+ d = 2n\pi$; from (26) we see that the phase of the contribution from this pole is of the form $-\mathrm{i}\sigma_n^+ x-\mathrm{i}\gamma(\sigma_n^+)y$, or in terms of axes aligned along the face of the cascade (see figure 1),

$$-\mathrm{i}(\sigma_n^+\sin\alpha-\gamma(\sigma_n^+)\cos\alpha)\,\tilde{x}-\mathrm{i}(\sigma_n^+\cos\alpha+\gamma(\sigma_n^+)\sin\alpha)\tilde{y} \equiv -\mathrm{i}K_{\tilde{x}}\,\tilde{x}-\mathrm{i}K_{\tilde{y}}\,\tilde{y},$$

where $K_{\tilde{x}}$ and $K_{\tilde{y}}$ are wavenumbers in the $\tilde{x}$- and $\tilde{y}$-directions respectively. From (19) we have

$$K_{\tilde{y}} = \frac{2n\pi-\sigma}{(d^2+s^2)^{\frac{1}{2}}}, \quad K_{\tilde{x}} = -K_{\tilde{y}}\cot\alpha+\frac{\sigma_n^+}{\sin\alpha}, \tag{27}$$

and hence that $\mathrm{Im}(K_{\tilde{x}}) = \mathrm{Im}(\sigma_\nu^+/\sin\alpha)$, which is positive since σ_n^+ lies in the upper half-plane. The waves associated with this pole therefore decay in the negative x'-direction, and hence satisfy (iii). Similar arguments apply to those poles $k = \sigma_n^+$ which satisfy $-\gamma(\sigma_n^+)s+\sigma+\sigma_n^+ d = 2n\pi$.

We proceed to calculate the pressure jump across the $n = 0$ blade by inverting Φ_0 for $x > 0$, and the solution will fall into two distinct parts, as follows. First, for $x > d$, we use the form of ϕ_0 given in (18), and close Γ in the lower half-plane. Pole contributions now arise from the $k = k_n^-$ and from $k = \Omega$. The various terms in $\phi_0(x,y)$ can be found; the contribution from $k = k_n^-$, $n = 0, 1, 2, \ldots$ is

$$\frac{\epsilon_n V_g \mathscr{K}^-(\Omega)\,[1-\exp(\mathrm{i}\sigma+\mathrm{i}k_n^- d+\mathrm{i}n\pi)]\cos(n\pi y/s)}{s(k_n^--\Omega)\,\mathscr{K}^-(k_n^-)\,[k_n^-\beta^2+M^2\Omega]}\exp(-\mathrm{i}k_n^- x), \tag{28}$$

where $\epsilon_0 = \frac{1}{2}$ and $\epsilon_n = 1$ for $n > 0$; and from $k = \Omega$,

$$\frac{-V_g\exp(\mathrm{i}\sigma+\mathrm{i}\Omega d-\mathrm{i}\Omega x)}{\gamma(\Omega)\sin(\gamma(\Omega)s)}[\cos[\gamma(\Omega)(y-s)]\exp(-\mathrm{i}\sigma-\mathrm{i}\Omega d)-\cos(\gamma(\Omega)y)], \tag{29}$$

and we find that $\gamma(\Omega) = -\mathrm{i}\Omega$. We can therefore write the scattered field $\phi_0(x,y)$ for $x > d$ in the form

$$\phi_0(x,y) = A_c f(y)\exp(-\mathrm{i}\Omega x)+\sum_{n=0}^{\infty} A_n\cos\left(\frac{n\pi y}{s}\right)\exp(-\mathrm{i}k_n^- x), \tag{30}$$

with A_c and $f(y)$ defined in (29) and A_n in (28). It can easily be checked that this solution satisfies boundary condition (i); in fact the mode corresponding to $k = \Omega$ (which represents the distorted gust as it is convected through the cascade at the mean-flow Mach number) entirely cancels the velocity of the incident gust, whilst the infinite sum (representing the right-travelling duct modes) has zero normal velocity on $y = 0$. In the case when $p = 0$, so that k_n^- is complex for all $n \geqslant 1$, all the duct modes (apart from the plane-wave mode $n = 0$) are non-propagating (i.e. are cut off) and exhibit rapid spatial decay with x; this is referred to as the *sub-resonant* condition by Mani & Horvay (1970). Alternatively, when p is non-zero, the first $p+1$ modes (including the $n = 0$ mode) are cut on, and propagate down the duct; the so-called *super-resonant* condition. Equation (30) could be used, together with (35), to calculate the pressure jump across the zeroth blade for $x > d$. However, a simpler derivation is possible from the first Wiener–Hopf equation (16); inversion of this

expression for $[P_0^1(k,0)]_-^+$ when $x<0$ leads to zero pressure jump; when $x>d$, we have

$$[p_0^1(x,0)]_-^+ = \sum_{n=0}^{\infty} \frac{-\mathrm{i}V_g \mathscr{K}^-(\Omega)\,\epsilon_n(-1)^n}{\mathscr{K}^-(k_n^-)\,(k_n^-\beta^2+M^2\Omega)s}[1-\exp(-\mathrm{i}\sigma-\mathrm{i}k_n^- d-\mathrm{i}n\pi)]^2 \times \exp(\mathrm{i}\sigma+\mathrm{i}k_n^- d-\mathrm{i}k_n^- x). \quad (31)$$

Second, we consider the portion of the blade $0<x\leqslant d$, and to do this we must treat the two terms in (18) separately. The first term can be inverted for all $x>0$ by closing the integration contour in the lower half-plane to give, in exactly the same way as before,

$$-\frac{V_g\cos[(s-y)\,\gamma(\Omega)]\exp(-\mathrm{i}\Omega x)}{\gamma(\Omega)\sin[s\gamma(\Omega)]} \cdot + \sum_{n=0}^{\infty} \frac{\epsilon_n V_g \mathscr{K}^-(\Omega)}{(k_n^--\Omega)\,\mathscr{K}^-(k_n^-)\,s(M^2\Omega+k_n^-\beta^2)}\cos(n\pi y/s)\exp(-\mathrm{i}k_n^- x). \quad (32)$$

For $x<d$ the second term cannot be inverted by closing in the lower half-plane; it is therefore rewritten in the form

$$\frac{-V_g \mathscr{K}^-(\Omega)\,\mathscr{K}^+(k)\cos(\gamma y)}{2(k-\Omega)^2\exp(-\mathrm{i}\sigma-\mathrm{i}kd)[\cos(\sigma+kd)-\cos(\gamma s)]}, \quad (33)$$

and inverted by closing in the upper half-plane, to give

$$\sum_{n=-\infty}^{\infty} \frac{\mathrm{i}V_g \mathscr{K}^-(\Omega)\,\mathscr{K}^+(\sigma_n^+)(2n\pi-\sigma-\sigma_n^+ d)\cos[\gamma(\sigma_n^+)y]\exp(\mathrm{i}\sigma+\mathrm{i}\sigma_n^+ d-\mathrm{i}\sigma_n^+ x)}{2(\sigma_n^+-\Omega)^2\sin(\sigma+\sigma_n^+ d)[2n\pi d-\sigma d-s^2M^2\Omega-\sigma_n^+(\beta^2s^2+d^2)]}. \quad (34)$$

An expression for the pressure jump across the zeroth blade for $0<x\leqslant d$ can now be calculated from (32) and (34) as

$$[p_0^1(x,0)]_-^+ = \sum_{n=0}^{\infty} \frac{\mathrm{i}\epsilon_n V_g \mathscr{K}^-(\Omega)}{\mathscr{K}^-(k_n^-)\,s(M^2\Omega+k_n^-\beta^2)}(2-\exp[-\mathrm{i}k_n^- d-\mathrm{i}\sigma-\mathrm{i}n\pi])\exp(-\mathrm{i}k_n^- x) + \sum_{n=-\infty}^{\infty} \frac{V_g \mathscr{K}^-(\Omega)\mathscr{K}^+(\sigma_n^+)(2n\pi-\sigma-\sigma_n^+ d)\exp(\mathrm{i}\sigma+\mathrm{i}\sigma_n^+ d-\mathrm{i}\sigma_n^+ x)}{2(\Omega-\sigma_n^+)\sin(\sigma+\sigma_n^+ d)[2n\pi d-\sigma d-s^2M^2\Omega-\sigma_n^+(\beta^2s^2+d^2)]}. \quad (35)$$

From (16), and the form of the split function given in §5, it can be seen that, in the limit $k\to\infty$ in R^+, $[P_0^1(k,0)]_-^+ \sim k^{-\frac{1}{2}}$; this yields the typical leading-edge pressure singularity, $[p_0^1(x,0)]_-^+ \sim x^{-\frac{1}{2}}$ as $x\to+0$. This fact becomes readily apparent from equation (35) by using Lighthill's (1958) theory of asymptotic Fourier series; it is the first infinite series in (35) which is singular at $x=0$, and the coefficients in this mode series behave like $n^{-\frac{1}{2}}$ as $n\to\infty$ (since $\mathscr{K}^-(k_n^-)\sim(k_n^-)^{-\frac{1}{2}}$ and $k_n^-\sim n$ as $n\to\infty$), corresponding to an $x^{-\frac{1}{2}}$ singularity.

We emphasize that the value of $[p_0^1(x,0)]_-^+$ in $\{0<x\leqslant d\}$ is given by (35), and in $x\geqslant d$ by (31). The physical reason that the pressure jump across the zeroth blade takes these differing functional forms on either side of $x=d$ is clear. For $x>d$ duct modes are supported both above and below the blade, so that the lift is generated purely by these duct mode contribution (i.e. (31)). Alternatively, for $x<d$, whilst duct modes exist below the zeroth blade none can exist above the blade (owing to the stagger of the cascade); above the blade the field is composed of radiated modes (i.e. σ_n^+), and

hence the pressure jump for $x < d$ contains both duct mode and radiated mode contributions (i.e. (35)). The continuity of $[p_0^1(x,0)]^{\pm}$ across $x = d$ is guaranteed by Cauchy's theorem, together with the fact that the second term in (18) multiplied by $\exp(-ikd)$ vanishes sufficiently rapidly at infinity in upper and lower half-planes. Equations (31) and (35), when evaluated at $x = d$, are simply two different representations of the same physical quantity; the former in terms of duct modes, and the latter in terms of radiating modes. In order to demonstrate the smoothness of our solution away from the leading edge (as required by differentiability theorems for elliptic equations) we note that the x-derivatives of the pressure jump at $x = d$ can only be found from (35) (and not from (31), the x-derivative of which diverges at $x = d$); this is apparent from the form of the Fourier transform in (18), since inversion of a k-multiple of the second term is only possible by closing Γ in the upper half-plane (i.e. (35)). Once this restriction has been made, the coefficients in the modal expansions of $[p_0^1(x,0)]^{\pm}$ are seen to decay exponentially with large n everywhere, except at $x = 0$, guaranteeing that our solution is infinitely differentiable away from the leading edge.

We have therefore calculated the pressure jump across the zeroth plate (and hence, via (5), across all the others) due to the initial scattering of the incident harmonic gust by the cascade leading edges. The convected-gust (Ω) and plane-wave (k_0^-) contributions will always propagate down the ducts between adjacent blades; at sufficiently high frequency other (higher-order) duct modes will also propagate. All these cut-on contributions will be scattered by the trailing edges, resulting in an additional pressure jump across the blades; this will be calculated in the next section by solving the trailing-edge problem for $\psi_0^{(1)}(x,y)$.

4. The trailing-edge problem

For convenience we set $x' = x - 1$ in what follows, and work with a new coordinate origin located at the trailing edge of the zeroth blade. The problem is to solve for $\psi_0^{(1)}(x',y)$ using the prescription described in §2; i.e. such that the total pressure jump due to $\phi_0^{(1)} + \psi_0^{(1)}$ is zero across $\{x' > 0, y = 0\}$, and such that $\psi_0^{(1)}$ has zero normal derivative on $\{x' < 0, y = 0\}$. This is equivalent to consideration of the scattering of duct modes (specified by $\phi_0^{(1)}$) by the trailing edges of the (semi-infinite) blades; whilst it will typically only be the cut-on duct modes in $\phi_0^{(1)}$ which interact with the trailing edge (since the cut-off modes are exponentially small downstream of $x = d$), we shall retain all the terms in (30) in our analysis, and thereby include consideration of the restricted set of parameter values for which the lowest-order cut-off mode, k_{p+1}^-, is only just cut-off (i.e. $\mathrm{Im}(k_{p+1}^-)$ is small) and will not have decayed significantly by the time it has reached the trailing edge.

The analysis proceeds in much the same way as in §3, and we again drop the superfix(1) in referring to the scattered fields. The Fourier transform of $\psi_0(x',y)$ is now given by

$$\Psi_0(k,y) = \int_{-\infty}^{\infty} \psi_0(x',y) \exp(ikx')\,dx', \tag{36}$$

which is again split into two terms, $\Psi_0^{\pm}(k,y)$, with semi-infinite ranges of integration $x' > 0$ and $x' < 0$ respectively. $\Psi_0(k,y)$ will satisfy (8), so that

$$\Psi_0(k,y) = C\exp(-i\gamma y) + D\exp(i\gamma y); \tag{37}$$

use of the periodicity condition (iv) (§2), together with the continuity of normal

velocity, yields a relation between C and D and an expression for $[P_0^{\mathrm{t}}(k,0)]_-^+$ (the Fourier transform of the pressure jump across $y=0$ associated with ψ_0, i.e. due to the trailing-edge scattering) in the form

$$[P_0^{\mathrm{t}}(k,0)]_-^+ = 2\mathrm{i}(k-\Omega)\,D[1-\exp(-\mathrm{i}\sigma-\mathrm{i}kd+\mathrm{i}\gamma s)]. \tag{38}$$

The half-range Fourier transform of the condition of zero pressure jump across $\{x' \geqslant 0, y=0\}$ yields

$$[P_0^{\mathrm{l},+}(k,0)]_-^+ + [P_0^{\mathrm{t},+}(k,0)]_-^+ = 0, \tag{39}$$

with the second $(+)$ superfix on P_0 indicating that the integrations have been completed over the semi-infinite interval $x'>0$, and that the quantities are therefore analytic in the upper half k-plane. It can be shown that

$$[P_0^{\mathrm{l},+}(k,0)]_-^+ = \mathrm{i}(k-\Omega)\,[\Phi_0^+(k,0)]_-^+ + \Delta, \tag{40}$$

where Δ is the jump in $\phi_0(x',y)$ across the trailing edge, i.e.

$$\Delta = \phi_0(x'=0,0) - \phi_{-1}(x'=0,0),$$

and expressions for Δ and for $[\Phi_0^+(k,0)]_-^+$ found from (30) (owing to the change in coordinate origin an additional phase factor must be included in $[\Phi_0^+(k,0)]_-^+$). An expression for the Fourier transform of $\partial\psi_0/\partial y$ is found from (37), and the condition of zero total normal velocity on the blade implies

$$\frac{\partial \Psi_0^-}{\partial y}(k,0) \equiv 0;$$

together these yield

$$\frac{\partial \Psi_0}{\partial y}(k,0) = \frac{2D\exp(-\mathrm{i}\sigma-\mathrm{i}kd)\,\gamma\sin(\gamma s)}{\exp(-\mathrm{i}\gamma s-\mathrm{i}\sigma-\mathrm{i}kd)-1} = \frac{\partial \Psi_0^+}{\partial y}(k,0), \tag{41}$$

and so by substituting (38), (40) and (41) into (39), and recalling the definition of $\mathscr{K}(k)$ (equation (15)), we have a Wiener–Hopf equation, which is written in the form

$$\begin{aligned} F(k) = \mathscr{K}^+(k)\frac{\partial \Psi_0^+}{\partial y}(k,0) + \sum_{n=0}^{\infty} \frac{A_n \exp(-\mathrm{i}k_n^-)}{k_n^- - k}\left(\frac{k_n^- - \Omega}{\mathscr{K}^-(k_n^-)}\right) \\ \times [1-\exp(-\mathrm{i}n\pi - \mathrm{i}k_n^- d - \mathrm{i}\sigma)] \qquad (42a) \\ = \frac{[P_0^{\mathrm{t},-}(k,0)]_-^+}{\mathscr{K}^-(k)} - \sum_{n=0}^{\infty} \frac{A_n \exp(-\mathrm{i}k_n^-)}{k_n^- - k}\left(\frac{k-\Omega}{\mathscr{K}^-(k)} - \frac{k_n^- - \Omega}{\mathscr{K}^-(k_n^-)}\right) \\ \times [1-\exp(-\mathrm{i}n\pi - \mathrm{i}k_n^- d - \mathrm{i}\sigma)] \\ - \frac{1}{\mathscr{K}^-(k)} \sum_{n=0}^{\infty} A_n \exp(-\mathrm{i}k_n^-)[1-\exp(-\mathrm{i}\sigma - \mathrm{i}k_n^- - \mathrm{i}n\pi)]. \qquad (42b) \end{aligned}$$

These two equations imply that $F(k)$ is regular in R^+ and R^- respectively, and therefore throughout the whole complex plane. The trailing-edge Kutta condition implies that the pressure jump and the normal velocity must be non-singular at $x'=0$ (see, for instance, Crighton 1985), and we therefore set $F \equiv 0$. We now have from (42a) that

$$\frac{\partial \psi_0}{\partial y}(x',0) \sim (x')^{\frac{1}{2}} \quad \text{as} \quad x' \to +0,$$

and from (42*b*) that

$$[p_0^{\mathrm{t}}(x',0)]^{+}_{-} \sim -\sum_{n=0}^{\infty} A_n \exp(-\mathrm{i}k_n^-)[1-\exp(-\mathrm{i}n\pi-\mathrm{i}k_n^- d-\mathrm{i}\sigma)]\mathrm{i}(k_n^- - \Omega) \quad \text{as } x' \to -0;$$

by comparison with (28) and (31) it can be seen that the total pressure jump is zero at the trailing edge, which is exactly as would be expected. The solution can now be completed; from (42*a*) and from (41) an expression for D can be found, so that

$$\Psi_0(k,y) = -\frac{1}{\gamma \sin(\gamma s)\mathscr{K}^+(k)}[\cos(\gamma s-\gamma y)-\exp(\mathrm{i}\sigma+\mathrm{i}kd)\cos(\gamma y)]$$
$$\times \sum_{n=0}^{\infty} A_n \frac{\exp(-\mathrm{i}k_n^-)[1-\exp(-\mathrm{i}n\pi-\mathrm{i}k_n^- d-\mathrm{i}\sigma)]}{\mathscr{K}^-(k_n^-)}\left(\frac{k_n^- - \Omega}{k_n^- - k}\right); \quad (43)$$

or alternatively, substituting $\mathscr{K}^-/\mathscr{K}^-$ for $\mathscr{K}^+$,

$$\Psi_0(k,y) = \frac{1}{\Omega-k}\left(\frac{\exp(-\mathrm{i}\gamma y)}{\exp(-\mathrm{i}\gamma s-\mathrm{i}\sigma-\mathrm{i}kd)-1}+\frac{\exp(\mathrm{i}\gamma y)}{\exp(\mathrm{i}\gamma s-\mathrm{i}\sigma-\mathrm{i}kd)-1}\right)$$
$$\times \sum_{n=0}^{\infty} \mathrm{i}A_n \frac{\exp(-\mathrm{i}k_n^-)[1-\exp(-\mathrm{i}n\pi-\mathrm{i}k_n^- d-\mathrm{i}\sigma)]\mathscr{K}^-(k)}{2\mathscr{K}^-(k_n^-)}\left(\frac{k_n^- - \Omega}{k_n^- - k}\right). \quad (44)$$

Recovery of $\psi_0(x',y)$ from $\Psi_0(k,y)$ is completed in much the same way as in the previous section, and we again consider the fields inside and outside the cascade separately. For $x' > 0$ (i.e. downstream of the trailing edge of the zeroth blade) we use (44), and close the inversion contour in the lower half-plane, and there will be terms arising from the poles at $k = k_n^-, n = 0, 1, 2\ldots$, at $k = \Omega$, and at $\sigma_n^-, n = 0, \pm 1, \pm 2\ldots$. The total contribution from all the k_n^- is

$$-\sum_{n=0}^{\infty} A_n \exp(-\mathrm{i}k_n^-)\cos(n\pi y/s)\exp(-\mathrm{i}k_n^- x'),$$

which by comparison with (30) is seen to exactly cancel the duct mode terms in $\phi_0(x',y)$, which is as expected since no duct modes could be supported in the free space behind the cascade. The contributions to the scattered field from $k = \sigma_n^-$ correspond to radiation in directions behind the cascade, and it can be shown that these terms satisfy the radiation condition (boundary condition (iii)) via the same arguments as those following (26). Finally, the pole contribution to $\psi_0(x,y)$ from $k = \Omega$ corresponds to that part of the scattered solution which is convected with the mean flow, and together with the term in (29) represents the vortex sheet shed by the trailing edge. It should be noted that the boundary condition of zero pressure jump in $\phi_0 + \psi_0$ across $\{x' > 0, y = 0\}$ is satisfied by our solution, since neither the convected part of the solution (which has zero associated pressure) nor the radiative terms (essentially because of the periodicity of the solution) contain a pressure jump across $y = 0$. We will not calculate the radiative terms (or the vorticity waves) in $x' < 0$, since our primary concern here is with the pressure jump across the blades.

Calculation of the pressure jump generated by the trailing-edge scattering must be completed separately in the two regions $x' \leqslant -d$ and $-d \leqslant x' \leqslant 0$, in parallel with the

leading-edge analysis. First, to recover $[p^t(x',0)]^+_-$ in $x' < -d$ we use (43), and close the inversion contour in the upper half-plane. There will now be pole contributions from the zeros of $\gamma \sin(\gamma s)$ in R^+ (i.e. at $k = k^+_m, m = 0, 1, 2, \ldots$); from $k = k^+_m$ there will be a contribution of

$$\frac{\mathrm{i}\epsilon_m}{s(k^+_m\beta^2 + M^2\Omega)\,\mathscr{K}^+(k^+_m)}[1 - \exp(\mathrm{i}\sigma + \mathrm{i}k^+_m d + \mathrm{i}m\pi)]\,S(k^+_m)$$

$$\times \cos(m\pi y/s)\exp(-\mathrm{i}k^+_m x'), \quad (45)$$

with $$S(k) \equiv \sum_{n=0}^{\infty} A_n \frac{\exp(-\mathrm{i}k^-_n)[1 - \exp(-\mathrm{i}n\pi - \mathrm{i}k^-_n d - \mathrm{i}\sigma)]}{\mathscr{K}^-(k^-_n)}\left(\frac{k^-_n - \Omega}{k^-_n - k}\right) \quad (46)$$

and we write ψ_0 in $x' < 0$ in the form

$$\psi_0(x', y) = \sum_{m=0}^{\infty} B_m \exp(-\mathrm{i}k^+_m x')\cos(m\pi y/s), \quad (47)$$

with the coefficients B_m given by (45) and (46). The pressure jump associated with ψ_0 across the zeroth blade for $x' < -d$ is then

$$[p^t_0(x',0)]^+_- = \sum_{m=0}^{\infty} \mathrm{i}B_m(k^+_m - \Omega)[1 - \exp(-\mathrm{i}\sigma - \mathrm{i}k^+_m d - \mathrm{i}m\pi)]\exp(-\mathrm{i}k^+_m x'). \quad (48)$$

Second, to recover $[p^t(x',0)]^+_-$ in $-d \leqslant x' \leqslant 0$ we invert the second term in (43) by closing the inversion contour in the upper half-plane as above. However, just as in §3, we must rewrite the first term in (43) in the form

$$\frac{\mathrm{i}\cos(\gamma s - \gamma y)\,\mathscr{K}^-(k)}{2(k - \Omega)[\cos(\gamma s) - \cos(\sigma + kd)]}S(k); \quad (49)$$

this is then inverted by closing the contour in the lower half-plane, with contributions from the poles at $k = \Omega, k = \sigma^-_n, n = 0, \pm 1, \pm 2, \ldots$ and at $k = k^-_n, n = 0, 1, 2, \ldots$. After some effort the pressure jump associated with ψ_0 in the region $-d \leqslant x' \leqslant 0$ is found to be

$$[p^t_0(x',0)] = \sum_{m=0}^{\infty} \frac{\mathrm{i}A_m(\Omega - k^-_m)\exp(-2\mathrm{i}\sigma - 2\mathrm{i}k^-_m d - \mathrm{i}k^-_m)}{1 - \exp(-\mathrm{i}\sigma - \mathrm{i}m\pi - \mathrm{i}k^-_m d)}\exp(-\mathrm{i}k^-_m x')$$

$$+ \sum_{m=0}^{\infty} \frac{\epsilon_m(k^+_m - \Omega)\,S(k^+_m)[\exp(\mathrm{i}\sigma + \mathrm{i}m\pi + \mathrm{i}k^+_m d) - 2]}{s(M^2\Omega + \beta^2 k^+_m)\,\mathscr{K}^+(k^+_m)}\exp(-\mathrm{i}k^+_m x')$$

$$- \sum_{m=0}^{\infty} \frac{\mathrm{i}\mathscr{K}^-(\sigma^-_m)(2m\pi - \sigma - \sigma^- m\,d)\,S(\sigma^-_m)\exp(-\mathrm{i}\sigma - \mathrm{i}\sigma^-_m d)}{2\sin(\sigma + \sigma^-_m d)[2m\pi d - \sigma d - M^2\Omega s^2 - \sigma^-_m(d^2 + s^2\beta^2)]}$$

$$\times \exp(-\mathrm{i}\sigma^-_m x'), \quad (50)$$

with $S(k)$ defined in (46). The pressure jump generated by the scattering of ψ_0 at the trailing edge (i.e. $[p^t_0(x',0)]^+_-$) is therefore given by (48) in the region $x' \leqslant -d$ (where the solution comprises contributions form duct modes), and by (50) in $-d \leqslant x' \leqslant 0$ (where the solution comprises contributions from radiated and duct modes). The

continuity and smoothness of $[p_0^1(x',0)]^{\pm}$ at $x'=-d$ can be demonstrated by use of exactly the same arguments as were applied in §3 for $[p_0^1(x,0)]^{\pm}$ at $x=d$.

The accuracy of our approach depends of course on the validity of neglecting the higher terms in the reflection series (6); from (45) it can in fact be seen that ψ_0 is a factor of $O(\Omega)$ smaller than ϕ_0 (since $\mathscr{K}^+(k_m^+)$ is $O(\Omega^{\frac{1}{2}})$ and $\mathscr{K}^-(k_n^-)$ is $O(\Omega^{-\frac{1}{2}})$). Similar analysis to that employed in this section could also be used to show that the reflection of ψ_0 by the leading edge is a further $O(\Omega)$ smaller; in the notation of §2 we have that $\phi_0^{(m)}$ and $\psi_0^{(m)}$ are $O(\Omega^2)$ smaller than $\phi_0^{(m-1)}$ and $\psi_0^{(m-1)}$ respectively. For high reduced frequency the truncation of (6) to just the first two terms therefore provides a good approximation, as would be expected on physical grounds, since the lengthscale of high-frequency radiation will be smaller than the cascade dimensions, so that the right-travelling duct modes can pass through the trailing-edge region with little reflection.

5. Asymptotic factorization of the Wiener–Hopf kernel function

The solution described above relies on the factorization of the Wiener–Hopf kernel function $\mathscr{K}(k)$ in the form $\mathscr{K}=\mathscr{K}^+\mathscr{K}^-$, where $\mathscr{K}^{\pm}(k)$ are analytic, non-zero and possess algebraic growth at infinity in the half-planes $R^{\pm}$ respectively. This has been achieved by other authors (see for instance Koch 1971 and Carlson & Heins 1946) by use of an infinite-product decomposition (see Appendix B of this paper); the disadvantage of this method, however, is that the computational time required to evaluate the infinite products becomes large (particularly at high frequency and when both the phase and the modulus of the product are required). A different approach will therefore be adopted here, and the factorization accomplished *asymptotically*, in the formal limit $\Omega\to\infty$. The resulting algebraic formulae will provide considerably more physical insight than the corresponding infinite-product expressions, will be easy to compute and will be seen to be valid even for relatively moderate values of Ω.

We begin by writing

$$\left.\begin{aligned}\mathscr{K}(k)&=\frac{2(\Omega-k)}{\gamma}\mathscr{J}(k),\\ \mathscr{J}(k)&=\frac{[1-\exp(\mathrm{i}\sigma+\mathrm{i}kd-\mathrm{i}\gamma s)][1-\exp(-\mathrm{i}\sigma-\mathrm{i}kd-\mathrm{i}\gamma s)]}{1-\exp(-2\mathrm{i}\gamma s)},\end{aligned}\right\}\tag{51}$$

where the first factor in $\mathscr{K}(k)$ is easy to factorize, and $\mathscr{J}(k)$ is the part which must be decomposed via asymptotic analysis. Integral expressions for the multiplicative decomposition factors of $\mathscr{J}(k)$ are given by Noble (1958), with

$$\mathscr{J}^-(k)=\exp\left[\frac{-1}{2\pi\mathrm{i}}\int_{\mathrm{i}c_--\infty}^{\mathrm{i}c_-+\infty}\frac{\ln\mathscr{J}(\xi)}{\xi-k}\,\mathrm{d}\xi\right];\tag{52}$$

the contour lies within the strip of overlap between R_+ and R_-, with $c_-\geqslant 0$ (note that, by construction, $\mathscr{J}(k)\to 1$ at ∞ in the strip). A similar expression exists for $\mathscr{J}^+(k)$.

In order to cast $\mathscr{J}^-(k)$ into a form suitable for asymptotic analysis, we now expand $\ln\mathscr{J}$ as a series of exponentials, using

$$\ln(1-x)=-\sum_{n=1}^{\infty}\frac{x^n}{n},\tag{53}$$

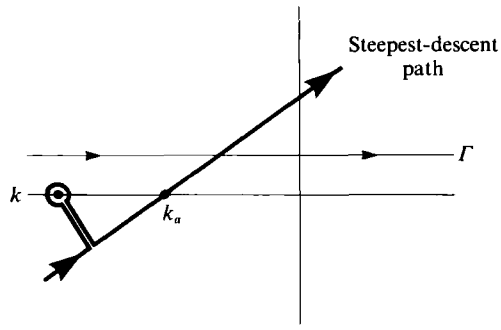

FIGURE 3. The deformation of the $\mathscr{K}^-$ contour Γ onto the steepest-descent path through k_a. In this case there will be a contribution from the pole at k on the real axis.

so that from (51)

$$\ln \mathscr{J}(\xi) = \sum_{n=1}^{\infty} \frac{1}{n} \{\exp(-2ins\gamma(\xi)) - \exp(in\sigma + in\xi d - ins\gamma(\xi)) - \exp(-in\sigma - in\xi d - ins\gamma(\xi))\}. \quad (54)$$

Equation (53) is of course only valid provided that $|x| \leqslant 1$ and $x \neq 1$; in the strip $R^+ \cap R^-$ we have $\mathrm{Im}(\gamma) < 0$, which guarantees that the modulus of each exponential term in (54) is strictly less than unity for k on the real axis, and our expansion in (54) is therefore valid provided we choose $c_- = +0$, i.e. the integration contour in (52) is the real axis indented above. The two expressions for $\ln \mathscr{J}$ (one being (54) and the other being found by taking the logarithm of (51)) therefore agree on the real axis, but are otherwise very different. We now factorize $\mathscr{J}(k)$ asymptotically, using the form for $\ln \mathscr{J}$ given in (51); this is essentially Koiter's (1954) method, whereby a function which is difficult to factorize (i.e. (51)) is represented over a limited region of the complex plane by a function whose factorization can be completed more easily (i.e. (54)). The validity of this approach is guaranteed by the fact that the $\mathscr{J}^{\pm}(k)$ factors are calculated from integrals in the strip $R^+ \cap R^-$, which is precisely where our two representations agree.

The analysis now proceeds by substituting (54) into (52), and it then remains to determine the leading terms in the large-Ω expansions of three integrals (denoted I_a, I_b and I_c, and defined in Appendix A). Full mathematical details are given in Appendix A; an outline of the analysis of I_a is given below (the expansion of I_b and I_c proceeds in much the same way). The problem, then, is the asymptotic evaluation of

$$I_a = \int \frac{\exp(-2ins\gamma(\xi))}{\xi - k} d\xi, \quad (55)$$

and as stated the integration contour is the real axis indented above. The argument of the exponential in (55) possesses a single saddle point at $\xi = k_a$ (equation (A 3)), so by deforming the contour onto the steepest-descent path through k_a, standard theory can be used to calculate the leading term in the asymptotic expansion of I_a. In addition, a contribution from the pole of the integrand at $\xi = k$ could also be present as a result of deforming the integration contour, and this will depend on the relative positions of the pole and the steepest-descent path (see figure 3). In the first instance if we suppose that k is real (i.e. the pole lies on the real axis), it is clear from

figure 3 that the pole contribution to I_a is picked up only if $k_a > k$. We therefore emphasize that there will always be a saddle point (steepest-descent) contribution to I_a, and possibly a pole contribution as well.

The asymptotic factorization of $\mathscr{J}(k)$ (and hence $\mathscr{K}(k)$) is now completed by use of the results from Appendix A; we eventually find that, for real k,

$$\mathscr{K}^-(k) \sim \frac{C^-}{[M\Omega+k(1-M)]^{\frac{1}{2}}}\exp\left[-\frac{1}{2\pi\mathrm{i}}\sum_{n=1}^{\infty}\frac{1}{n}\right.$$

$$\times\left\{\left(\frac{\pi M\Omega}{ns\beta^3}\right)^{\frac{1}{2}}\exp(\tfrac{1}{4}\pi\mathrm{i})\frac{\exp[-2ins\gamma(k_a)]}{k_a-k}\right.$$

$$-\left(\frac{2\pi M\Omega}{ns\Lambda^{\frac{3}{2}}}\right)^{\frac{1}{2}}\exp(\tfrac{1}{4}\pi\mathrm{i})\frac{\exp[in\sigma+indk_b-ins\gamma(k_b)]}{k_b-k}$$

$$\left.\left.-\left(\frac{2\pi M\Omega}{ns\Lambda^{\frac{3}{2}}}\right)^{\frac{1}{2}}\exp(\tfrac{1}{4}\pi\mathrm{i})\frac{\exp[-in\sigma-indk_c-ins\gamma(k_c)]}{k_c-k}\right\}\right]$$

$$\times\frac{[1-\mathrm{H}(k_b-k)\exp(\mathrm{i}\sigma+\mathrm{i}kd-\mathrm{i}s\gamma(k))][1-\mathrm{H}(k_c-k)\exp(-\mathrm{i}\sigma-\mathrm{i}kd-\mathrm{i}s\gamma(k))]}{[1-\mathrm{H}(k_a-k)\exp(-2\mathrm{i}s\gamma(k))]}; \tag{56}$$

the quantities k_a, k_b, k_c and Λ are defined in Appendix A, $\mathrm{H}(k)$ is the Heaviside step function, and the arbitrary constant C^- is chosen for normalization purposes (C^- is chosen so that $\mathscr{K}^-(z_0) = 1$ for some fixed z_0, and z_0 will usually be taken as zero). The first factor in (56) arises from (51), the exponential factor whose argument is an infinite sum arises from the saddle point contributions to the various integrals, and the factors containing the step functions arise from the pole contributions (the argument of one of the H being positive corresponds to a pole contribution having been picked up in one of I_a, I_b and I_c). In deriving this expression for $\mathscr{K}^-(k)$ the small imaginary part of Ω has been set equal to zero.

An asymptotic expression for $\mathscr{K}^+(k)$ can be found in much the same way, and is (for real k)

$$\mathscr{K}^+(k) \sim \frac{C^+(\Omega-k)}{[M\Omega-k(1+M)]^{\frac{1}{2}}}\exp\left[+\frac{1}{2\pi\mathrm{i}}\sum_{n=1}^{\infty}\frac{1}{n}\right.$$

$$\times\left\{\left(\frac{\pi M\Omega}{ns\beta^3}\right)^{\frac{1}{2}}\exp(\tfrac{1}{4}\pi\mathrm{i})\frac{\exp[-2ins\gamma(k_a)]}{k_a-k}\right.$$

$$-\left(\frac{2\pi M\Omega}{ns\Lambda^{\frac{3}{2}}}\right)^{\frac{1}{2}}\exp(\tfrac{1}{4}\pi\mathrm{i})\frac{\exp[in\sigma+indk_b-ins\gamma(k_b)]}{k_b-k}$$

$$\left.\left.-\left(\frac{2\pi M\Omega}{ns\Lambda^{\frac{3}{2}}}\right)^{\frac{1}{2}}\exp(\tfrac{1}{4}\pi\mathrm{i})\frac{\exp[-in\sigma-indk_c-ins\gamma(k_c)]}{k_c-k}\right\}\right]$$

$$\times\frac{[1-\mathrm{H}(k-k_b)\exp(\mathrm{i}\sigma+\mathrm{i}kd-\mathrm{i}s\gamma(k))][1-\mathrm{H}(k-k_c)\exp(-\mathrm{i}\sigma-\mathrm{i}kd-\mathrm{i}s\gamma(k))]}{[1-\mathrm{H}(k-k_a)\exp(-2\mathrm{i}s\gamma(k))]}; \tag{57}$$

here C^+ is chosen so that $\mathscr{K}^+(z_0) = \mathscr{K}(z_0)$, and it is easy to verify that (56) and (57) multiply together exactly to give the correct value of $\mathscr{K}(k)$ (equation (51)).

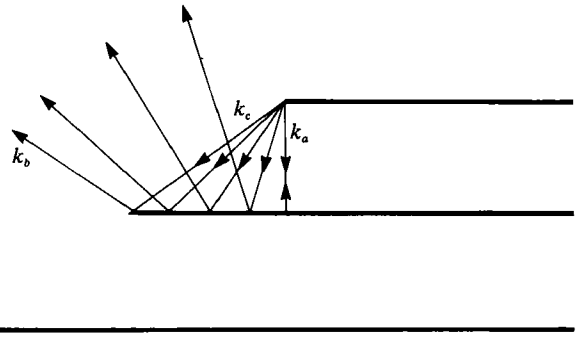

FIGURE 4. Scattered rays, emitted by a leading edge and reflected by the lower blade.

The physical interpretation of these expression follows by use of the dispersion relation for (2), i.e.

$$(M\Omega - Mk)^2 = k^2 + \gamma^2, \tag{58}$$

in calculating the group velocity of waves in the system; δ, the angle a ray with wave vector (k, γ) makes with the x-axis, is found to be

$$\delta = \tan^{-1}\left(\frac{\gamma}{\beta^2 k + M^2\Omega}\right). \tag{59}$$

From (A 3) it is clear that $\beta^2 k_a + M^2\Omega = 0$, and therefore that δ_a (the angle of the ray corresponding to the wavenumber k_a) is precisely $\frac{1}{2}\pi$. Similarly, from (A 8) and (A 13) we have $\delta_b = \pi - \alpha$ and $\delta_c = \alpha$, where α is the stagger angle of the cascade. Wavenumber k_c therefore corresponds to a ray travelling parallel to the front face of the cascade; k_b represents the reflection of this ray from a plate; and k_a represents the ray parallel to the y-axis.

In analogy to the Sommerfeld diffraction problem for an isolated plate, the saddle point contributions to the integrals I_a, I_b and I_c found above correspond to radiation scattered by the blade leading edges, whilst the pole contributions correspond to the geometrical optics component of the field. Given that $k_b < k_a < k_c$ (but that $\delta_c < \delta_a < \delta_b$), it can be seen in, for example, (57) that for wavenumbers k lying between k_b and k_a (i.e. ray directions lying in between δ_b and δ_a) there is a contribution to $\mathscr{K}^+(k)$ of a factor $[1 - \exp(i\sigma + ikd - is\gamma)]$; this contribution corresponds to rays originally emitted by the leading edge, and subsequently reflected by the lower blade. For $k > k_a$ (ray directions behind $\delta = \delta_a$) a second contribution is cut on, which, again in analogy to the Sommerfeld problem, acts to (partially) cancel this reflected contribution (this cancellation is only partial since the region of space in which $k > k_a$ will receive radiation from other blades, and is therefore not a genuine shadow zone). Wavenumbers k_b and k_a are therefore seen to represent the geometrical optics shadow boundaries – rays corresponding to waves reflected by a given blade only propagate in directions between these boundaries – whilst k_c represents a ray which travels along the front face of the cascade. This is made clear in figure 4.

For certain parameter values, (56) and (57) will no longer remain valid, however, due to the pole at k lying close to one of the saddle points. This effect, corresponding to the proximity of a ray to a shadow boundary, has been considered in other physical situations by a number of authors (see Crighton 1971; Jones 1986), and uniform formulae could indeed be derived in our case, involving a complex error

function. Such uniform analysis would reveal that the transition across the shadow boundaries is in fact a smooth one (with the transition region having a width of $O(\Omega^{-\frac{1}{3}})$), and not the step-function jump predicted by the outer solution in (56) and (57). However, the effort required in completing such calculations (particularly in view of the time-consuming computation of the various special functions) is hardly justified for the isolated instances in which it is needed; in our prediction scheme we shall therefore use the formulae given above where appropriate, and employ the infinite-product factorization of Appendix B in a very small number of special cases. We also note that when one of the saddle points approaches the origin we can no longer normalize $\mathscr{K}^{\pm}(k)$ by choosing $z_0 = 0$ (see following (56)), since this would also involve the uniform asymptotic analysis in evaluating $\mathscr{K}^{\pm}(0)$, and we must therefore make some alternative choice of z_0 (which lies sufficiently far from k_a, k_b and k_c, and which does not coincide with a zero or pole of $\mathscr{K}(k)$) in such cases.

As has been seen from the previous two sections, values of $\mathscr{K}^{\pm}(k)$ for both cut-on and cut-off modes $k = k_n^{\pm}, \sigma_n^{\pm}$ will be required, and the above procedure for real k (cut-on modes) can be generalized to include evaluation of $\mathscr{K}^{\pm}(k)$ for values of k lying off the real axis (cut-off modes) as well. The saddle point contributions will be found in exactly the same way as above; which pole contributions are to be included will depend on the relative positions of the poles and steepest-descent contours, and this is best determined graphically, or by simple numerical calculations involving (A 5) and (A 10). Modification to include the possibility of the poles approaching the saddle points for complex k is required, but the infinite product results will again be used in such special cases.

6. Results

We shall first demonstrate the accuracy of our asymptotic factorization method by comparing values for the Wiener–Hopf factors calculated using the equations derived in the previous section with the exact infinite-product results presented in Appendix B. We consider throughout the parameters $M = 0.8$, $\sigma = \frac{2}{3}\pi$, $d = \frac{1}{2}$ and $s = \frac{1}{2}\sqrt{3}$ (corresponding to a stagger angle of $\alpha = \frac{1}{3}\pi$ and a separation of 1 between the leading edges of adjacent blades), and illustrate the application of the method in detail by first taking $\Omega = 15$; these values might typically be encountered in an advanced contra-fan engine operating under cruise conditions. A relatively large number of modes will be cut-on, with $p = 5$, $q = 2$ and $r = 5$ (cf. (22) and (24)).

We describe here the calculation of $\mathscr{K}^{-}(k)$ for the wavenumbers $k = k_n^{-}$ and $k = \Omega$; determination of $\mathscr{K}^{-}(\sigma_n^{-})$ follows in much the same way. The positions in the complex plane of the k_n^{-} for $n = 0, \ldots, 12$, and of Ω, together with the steepest-descent paths defined in Appendix A, are shown in figure 5. The numerical values of these wavenumbers are given in table 1; we also note that the saddle points k_a, k_b and k_c are -26.667, -49.780 and -3.554 respectively. As described in the previous section, in order to determine $\mathscr{K}^{-}(k)$ asymptotically the $\mathscr{K}^{-}$ integration contour (i.e the real axis indented above) is deformed onto each of the three steepest-descent paths in turn. Considering first the calculation of $\mathscr{K}^{-}(k_n^{-})$, it is clear from figure 5 that a pole contribution is only picked up when deforming onto the c-contour, and then only for $n = 4, 5, 6, 7$. No pole contributions are present for $\mathscr{K}^{-}(\Omega)$.

The pole at $k = k_4^{-}$ lies in close proximity to the saddle point k_c, and in this isolated case the asymptotic formula of §5 is inapplicable and the error-function modification would be required. However, our formulae can readily be applied to all the remaining wavenumbers, and a comparison of the asymptotic and (exact) infinite-product

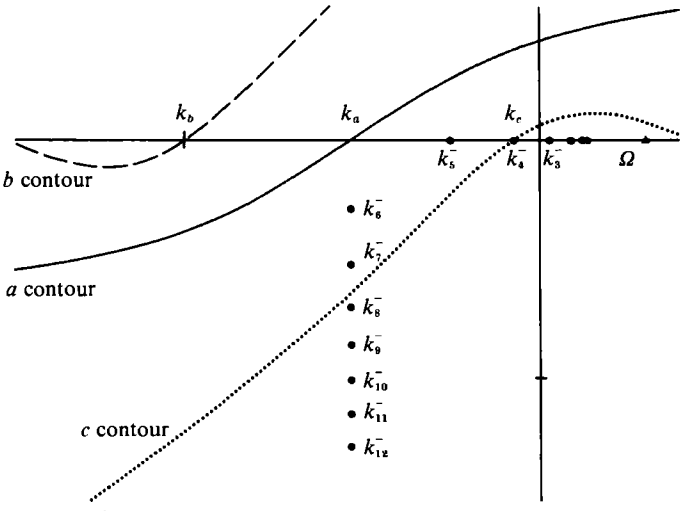

FIGURE 5. The steepest-descent curves for $\Omega = 15$; other parameters are $M = 0.8$, $d = \frac{1}{2}$, $s = \frac{1}{2}\sqrt{3}$ and $\sigma = \frac{2}{3}\pi$. The k_n^- modes (●) for $0 \leqslant n \leqslant 12$ and $k = \Omega$ (△) are also shown. Pole contributions are picked up when deforming the c contour for k_4^-, k_5^-, k_6^- and k_7^-.

		$\mathscr{K}^-(k_n^-)$		
n	k_n^-	Infinite product	Asymptotic	|Relative error|
0	6.667	0.169–0.865i	0.183–0.881i	2.44×10^{-2}
1	6.144	0.181–0.859i	0.199–0.877i	2.94×10^{-2}
2	4.396	0.220–0.832i	0.260–0.856i	5.41×10^{-2}
3	1.299	0.296–0.733i	0.450–0.733i	1.95×10^{-1}
4	−3.727	0.304–0.355i	*	*
5	−12.624	−1.238–0.220i	−1.214–0.155i	5.45×10^{-2}
6	−26.667–14.315i	−0.160–1.202i	−0.179–1.223i	2.30×10^{-2}
7	−26.667–26.080i	0.084–1.144i	0.088–1.169i	2.25×10^{-2}
8	−26.667–35.050i	0.199–1.060i	0.207–1.087i	2.58×10^{-2}
9	−26.667–43.011i	0.262–0.987i	0.271–1.014i	2.77×10^{-2}
10	−26.667–50.443i	0.299–0.925i	0.309–0.952i	2.94×10^{-2}
11	−26.667–57.552i	0.321–0.872i	0.332–0.899i	3.01×10^{-2}
12	−26.667–64.444i	0.335–0.827i	0.345–0.853i	3.10×10^{-2}
Ω	15	0.055–i0.878	0.055–0.880i	2.73×10^{-3}

TABLE 1. A comparison between the infinite-product (exact) and asymptotic values for $\mathscr{K}^-(k)$ evaluated at the duct modes $k = k_n^-$ and at $k = \Omega$, with $\Omega = 15$; other parameters are $M = 0.8$, $\sigma = \frac{2}{3}\pi$, $d = \frac{1}{2}$ and $s = \frac{1}{2}\sqrt{3}$. * indicates that the error-function modification would be required in order to obtain the asymptotic value.

values is given in table 1. As can be seen, excellent agreement is obtained, with the absolute value of the relative error in the asymptotic result being typically of the order of 2% or less (in the case of k_3^- a rather larger error is found, due to the relative proximity of the saddle at k_c, but this is still an acceptable level of accuracy in the context of asymptotic approximations, and has no practical effect on our final results). The most striking difference between the two methods is of course the fact that the asymptotic expressions were calculated relatively quickly, whilst the infinite-product expressions proved considerably more time-consuming (in order to guarantee convergence of the infinite products, especially for the higher wave-

numbers, as many as 6000 terms were required). In table 2 the comparison made in table 1 is repeated, but this time with the much lower reduced frequency of $\Omega = 5$, and good agreement is still obtained, with the typical error being of the order of 2% or less (a larger error is found in the case of wavenumber k_2^-, due to the relative proximity of the saddle k_a). Evaluation of $\mathscr{K}^+(k)$ follows in the same way as described above.

Having established the accuracy of our approximations to the split functions, we now proceed to substitute the asymptotic values of $\mathscr{K}^\pm(k)$ into our algebraic expressions for the unsteady lift distribution ((31), (35), (48) and (50)), using the infinite-product results only at those relatively few special-case wavenumbers for which our asymptotic formulae are invalid. In figure 6(*a–d*) the real and imaginary parts of the unsteady lift distribution along the chord are presented for $\Omega = 20, 15, 10, 5$; the oscillatory nature of the lift is exactly as one might expect at high frequency; the leading-edge inverse square-root singularity is clearly present; and the smoothness of the lift distribution at $x = \frac{1}{2}$ (for this choice of parameter values the point at which the modal expansions of both ϕ_0 and ψ_0 change form) is demonstrated (the very small discontinuity evident in the plot of the real part of the pressure jump in figure 6*d* is a result purely of the asymptotic approximation to the Wiener–Hopf factors, and is of no practical significance). We emphasize that, in order to resolve the leading-edge singularity and to ensure that the plots are smooth, $\mathscr{K}^\pm(k)$ must be calculated for considerably more wavenumbers than are displayed in table 1 (for instance, in calculating the first series in (35) the first 100 terms were included). Application of the infinite-product factorization method throughout would therefore prove prohibitively time-consuming, but the use of our asymptotic factorization scheme means that the whole calculation can be performed with use of only limited computer resource.

7. Concluding remarks

In this paper an asymptotic method has been developed for predicting the unsteady lift on a blade row due to the interaction with a convected vorticity wave. The high-frequency approximation has facilitated two simplifications; first the infinite reflection series has been legitimately truncated to just two terms, and second closed-form algebraic expressions for the Wiener–Hopf factors have been found (the accuracy of the latter having been demonstrated by comparison with exact factorization methods). The pressure jump comprises an infinite sum of mode contributions, with the form of the modal representation depending on the chordwise position, and is seen to possess the characteristic $x^{-\frac{1}{2}}$ singularity at the leading edge and to obey a trailing-edge Kutta condition. A number of interesting features, such as the presence of shadow boundaries, are also revealed, and our formulae are in a form which can be used to yield useful algebraic scaling laws on the major design parameters.

The value of our asymptotic approach lies in the fact that existing numerical techniques can prove unsatisfactory for the high-frequency cases encountered in ultra-high bypass ratio engines, but for which cascade effects can still be highly significant. The relative simplicity of the scheme should allow its extension to include blade camber and thickness, and to model other effects such as rotor blockage, and work is now well under way in this direction.

The author is very grateful to A. M. Cargill for suggesting this problem, and to

		$\mathscr{K}^-(k_n^-)$		
n	k_n^-	Infinite product	Asymptotic	|Relative error|
0	2.222	−0.278–2.268i	−0.131–2.223i	6.74×10^{-2}
1	0.433	−0.735–2.151i	*	*
2	−8.889–4.772i	1.362–4.863i	1.149–4.395i	1.02×10^{-1}
3	−8.889–14.337i	1.506–3.166i	1.549–3.162i	1.24×10^{-2}
4	−8.889–21.481i	1.515–2.542i	1.555–2.562i	1.52×10^{-2}
5	−8.889–28.115i	1.459–2.170i	1.494–2.194i	1.65×10^{-2}
6	−8.889–34.534i	1.390–1.918i	1.424–1.944i	1.82×10^{-2}
7	−8.889–40.839i	1.320–1.741i	1.356–1.761i	1.91×10^{-2}
8	−8.889–47.076i	1.258–1.599i	1.295–1.620i	2.07×10^{-2}
9	−8.889–53.269i	1.203–1.485i	1.239–1.508i	2.23×10^{-2}
10	−8.889–59.432i	1.153–1.392i	1.190–1.415i	2.41×10^{-2}
11	−8.889–65.573i	1.108–1.313i	1.145–1.338i	2.57×10^{-2}
12	−8.889–71.698i	1.068–1.246i	1.105–1.271i	2.73×10^{-2}
Ω	5	−0.038–2.433i	−0.063–2.470i	1.82×10^{-2}

TABLE 2. A comparison between the infinite-product (exact) and asymptotic values for $\mathscr{K}^-(k)$ evaluated at the duct modes $k = k_n^-$ and at $k = \Omega$, with $\Omega = 5$ and other parameters as in table 1

D. G. Crighton for illuminating discussions. The work was supported by an SERC studentship and by Rolls-Royce plc.

Appendix A

In this appendix we present the details of the asymptotic factorization of the Wiener–Hopf function $\mathscr{K}(k)$. By substituting (54) into (52), and noting that the infinite series are uniformly convergent for integration contours in the strip $R^+ \cap R^-$, we have

$$\mathscr{K}^-(k) = \exp\left[-\frac{1}{2\pi i}\sum_{n=1}^{\infty}\frac{1}{n}\left\{\int\frac{\exp(-2ins\gamma(\xi))}{\xi-k}\,d\xi - \int\frac{\exp(in\sigma+in\xi d-ins\gamma(\xi))}{\xi-k}\,d\xi - \int\frac{\exp(-in\sigma-in\xi d-ins\gamma(\xi))}{\xi-k}\,d\xi\right\}\right]; \quad \text{(A 1)}$$

it follows that we have essentially three integrals to expand asymptotically, and this will be completed formally in the limit $\Omega_r \to \infty$ (Ω_r is the real part of Ω), with Ω_i (the imaginary part of Ω) small and held fixed.

(*a*) The first term is

$$I_a = \int\frac{\exp(-2ins\gamma(\xi))}{\xi-k}\,d\xi, \quad \text{(A 2)}$$

where the contour of integration is the real axis, indented above the pole. For convenience, we first make the substitution $\xi' = \xi/\Omega_r$, and note that there is a single saddle point in the argument of the exponential at $\xi' = k_a/\Omega_r$, where

$$k_a = -\frac{M^2\Omega}{\beta^2}; \quad \text{(A 3)}$$

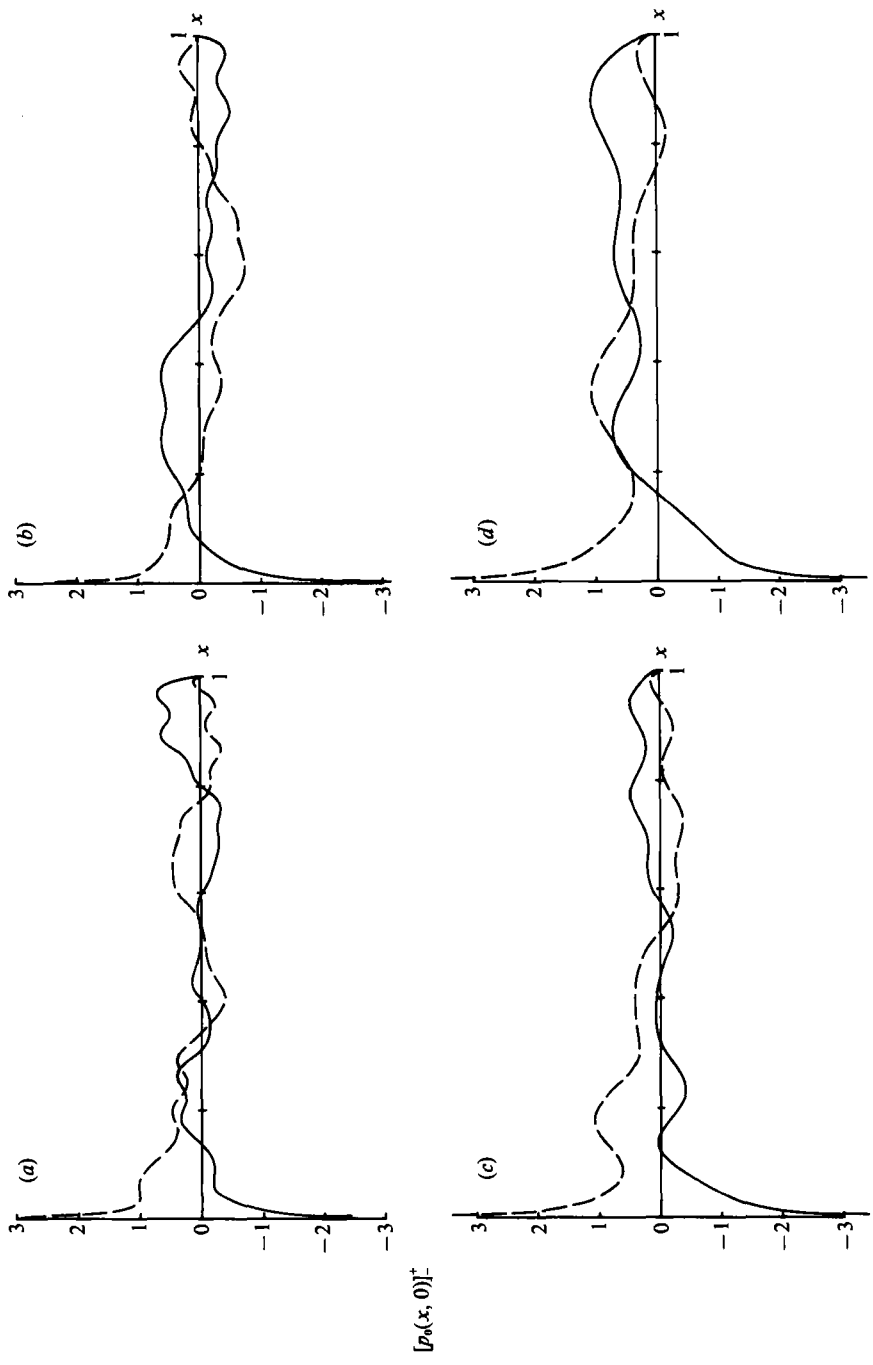

FIGURE 6. The real (solid line) and imaginary (broken line) parts of the chordwise lift distribution on the zeroth blade (i.e. in our asymptotic theory the quantity $[p_0'(x,0)]^+_- + [p_0^t(x,0)]^+_-$) is normalized by $\rho_0 V_g U$ and plotted against chordwise coordinate x running from 0 at the leading edge to 1 at the trailing edge. The values of the reduced frequency, Ω, are: (*a*) 20, (*b*) 15, (*c*) 10 and (*d*) 5. Other parameters are as in figure 5.

given that, in the asymptotic limit, Ω_i/Ω_r can be neglected compared to unity (so that we can effectively set $\Omega_i = 0$) we have that

$$\gamma(k_a) = \frac{M\Omega}{\beta}, \quad \frac{\mathrm{d}^2\gamma}{\mathrm{d}\xi^2}(k_a) = -\frac{\beta^3}{M\Omega}. \tag{A 4}$$

The equation of the steepest-descent path in the ξ' plane can be found in parametric form:

$$\xi' = t + \mathrm{i}\,\mathrm{Im}(\xi'),$$

with t real and

$$\mathrm{Im}(\xi') = \frac{(M/\beta)+\beta t}{[\beta^2(1+M^2)+\beta^6 t^2+2\beta^4 Mt]^{\frac{1}{2}}}. \tag{A 5}$$

The integration contour in (A 2) is now deformed onto the steepest-descent path through k_a (making an angle of $\frac{1}{4}\pi$ with the real axis at the saddle point), with the possibility of a contribution from the pole at $\xi = k$ (this is made clear in figure 3). In the first instance we suppose that k is real, so that the pole is picked up if $k_a > k$; standard asymptotic theory now yields the first term in the asymptotic expansion of I_a for real k, i.e.

$$I_a \sim \left(\frac{\pi M\Omega}{nh\beta^3}\right)^{\frac{1}{2}} \exp(\tfrac{1}{4}\pi\mathrm{i}) \frac{\exp[-2\mathrm{i}ns\gamma(k_a)]}{k_a - k} + 2\pi\mathrm{i}\,\mathrm{H}(k_a-k)\exp[-2\mathrm{i}ns\gamma(k)], \tag{A 6}$$

where $\mathrm{H}(k)$ is just the Heaviside step function. The continuation of this asymptotic expression for values of k off the real axis is straightforward; the first term in (A 6) is unchanged, whilst in the second term the step function is replaced by the function whose value is 1 when the pole at $\xi = k$ is picked up by deforming the integration contour, and 0 otherwise (an algebraic condition for inclusion of the pole contribution can easily be derived from (A 5).

(*b*) The second term to be evaluated asymptotically is

$$I_b = \int \frac{\exp(\mathrm{i}n\sigma + \mathrm{i}n\xi d - \mathrm{i}ns\gamma(\xi))}{\xi - k}\,\mathrm{d}\xi; \tag{A 7}$$

again making the substitution $\xi' = \xi/\Omega_r$, we find that the saddle point is $\xi' = k_b/\Omega_r$, with

$$k_b = -\frac{M^2\Omega}{\beta^2} - \frac{\Lambda^{-\frac{1}{2}}M\Omega\cot\alpha}{\beta^2} \tag{A 8}$$

and

$$\gamma(k_b) = M\Omega\Lambda^{-\frac{1}{2}} \tag{A 9}$$

where α is the blade stagger angle and

$$\Lambda = \beta^2 + \cot^2\alpha.$$

The steepest-descent path in the ξ' plane through this saddle point is given by

$$\left.\begin{aligned} \mathrm{Re}(\xi') &= t, \\ [\mathrm{Im}(\xi')]^2 &= \frac{-s^2 + 2Ms^2t + s^2\beta^2t^2 + [d(-t+k_b/M\Omega) - s\Lambda^{-\frac{1}{2}}]^2}{s^2\beta^2 + \left(\dfrac{Ms^2 + s^2\beta^2 t}{d(-t+k_b/M\Omega) - s\Lambda^{-\frac{1}{2}}}\right)^2}, \end{aligned}\right\} \tag{A 10}$$

with the value of the square root of (A 10) chosen to yield a smooth contour. It is easy

to show that this steepest-descent path also makes an angle of $\frac{1}{4}\pi$ to the real axis. The same procedure as in part (*a*) now yields, for real k,

$$I_b \sim \left(\frac{2\pi M\Omega}{nsA^{\frac{3}{2}}}\right)^{\frac{1}{2}} \exp(\tfrac{1}{4}\pi\mathrm{i}) \frac{\exp[\mathrm{i}n\sigma + \mathrm{i}nk_b d - \mathrm{i}ns\gamma(k_b)]}{k_b - k} + 2\pi\mathrm{i}H(k_b - k)\exp[\mathrm{i}n\sigma + \mathrm{i}nkd - \mathrm{i}ns\gamma(k)], \quad \text{(A 11)}$$

and extension to complex k is made just as above.

(*c*) The third term is

$$I_c = \int \frac{\exp(-\mathrm{i}n\sigma - \mathrm{i}n\,\mathrm{d}\xi - \mathrm{i}ns\gamma(\xi))}{\xi - k}\mathrm{d}\xi; \quad \text{(A 12)}$$

here the saddle point in the ξ' plane is $\xi' = k_c/\Omega_r$, where

$$k_c = -\frac{M^2\Omega}{\beta^2} + \frac{A^{-\frac{1}{2}}M\Omega\cot\alpha}{\beta^2}, \quad \text{(A 13)}$$

and we have $\gamma(k_c) = \gamma(k_b)$; the steepest-descent path is obtained simply by sending $\sigma \to -\sigma$ and $d \to -d$ in (A 10). It follows, again for real k, that

$$I_c \sim \left(\frac{2\pi M\Omega}{nsA^{\frac{3}{2}}}\right)^{\frac{1}{2}} \exp(\tfrac{1}{4}\pi\mathrm{i}) \frac{\exp[-\mathrm{i}n\sigma - \mathrm{i}nk_c d - \mathrm{i}nd\gamma(k_c)]}{k_c - k} + 2\pi\mathrm{i}H(k_c - k)\exp[-\mathrm{i}n\sigma - \mathrm{i}nkd - \mathrm{i}ns\gamma(k)]. \quad \text{(A 14)}$$

Appendix B

For completeness, and as a means of testing the accuracy of our asymptotic estimates, we describe the exact infinite-product factorization of $\mathscr{K}(k)$ in this Appendix – this has been present in slightly different forms by a number of other authors (see for instance Koch 1971).

Our starting point is the decomposition (Abramowitz & Stegun 1968)

$$\sin\alpha = \alpha \prod_{n=1}^{\infty}\left[1 - \left(\frac{\alpha}{n\pi}\right)^2\right], \quad \text{(B 1)}$$

which is employed in writing

$$\cos\gamma s - \cos(\sigma + kd) = \tfrac{1}{2}\sigma_0^+\sigma_0^-(d^2 + s^2\beta^2)\left(\prod_{-\infty,\, n\neq 0}^{\infty}\left[\frac{(d^2 + s^2\beta^2)}{4n^2\pi^2}\sigma_n^+\sigma_n^-\right]\right)\prod_{n=-\infty}^{\infty}\left(1 - \frac{k}{\sigma_n^+}\right)\left(1 - \frac{k}{\sigma_n^-}\right), \quad \text{(B 2)}$$

where the σ_n are the zeros of $\mathscr{K}(k)$, as defined earlier, and a similar result can easily be deduced for $\gamma\sin\gamma s$. Now, by considering $\mathscr{K}(k)$ in the form

$$\mathscr{K}(k) = \frac{2(\Omega - k)}{\mathrm{i}\gamma\sin\gamma s}[\cos\gamma s - \cos(\sigma + kd)], \quad \text{(B 3)}$$

an infinite-product expression for $\mathscr{K}^+(k)$ can be found, containing those factors corresponding to the zeros and poles of $\mathscr{K}(k)$ which lie in the lower half-plane, so that

$$\mathscr{K}^+(k) = N^+\frac{(1 - k/\sigma_0^-)(1 - k/\Omega)}{(1 - k/k_0^-)}\exp[-\chi(k)]\frac{\prod_{n=1}^{\infty}(1 - k/\sigma_n^-)\prod_{n=-1}^{-\infty}(1 - k/\sigma_n^-)}{\prod_{n=1}^{\infty}(1 - k/k_n^-)}. \quad \text{(B 4)}$$

Here, $\chi(k)$ is arbitrary, but will subsequently be chosen so that $\mathscr{K}^+(k)$ has algebraic behaviour at infinity in the upper half-plane, and the multiplicative constant N^+ has been included so that $\mathscr{K}^+(z_0) = \mathscr{K}(z_0)$ (z_0 will be chosen for convenience, and will often be zero); once this has been done, $\mathscr{K}^+(k)$ is uniquely determined.

In order to calculate χ we follow Noble's (1958) procedure for analysing the asymptotic behaviour of infinite products. We first note that, for a general infinite product with $a_n \sim an+b$ as $n \to \infty$,

$$\prod_{n=1}^{\infty} \frac{(1-z/a_n)\exp(z/a_n)}{(1-z/(an+b))\exp(z/an)} = \exp\left(z\sum_{n=0}^{\infty}\frac{1}{a_n}-\frac{1}{an}\right)\prod_{n=1}^{\infty}\left(\frac{an+b}{a_n}\right)\prod_{n=1}^{\infty}\left(\frac{a_n-z}{an+b-z}\right); \tag{B 5}$$

given the large-n behaviour of a_n, the first product on the right is convergent, whilst, in the limit of large z, the second product approaches unity. Application of the standard results (Abramowitz & Stegun 1968)

$$\frac{1}{\Gamma(z)} = z\exp(Ez)\prod_{n=1}^{\infty}\left[\left(1+\frac{z}{n}\right)\exp(-z/n)\right] \tag{B 6}$$

$$\frac{\Gamma(1+b/a)}{\Gamma(1+[-z+b]/a)} = \exp(-Ez/a)\prod_{n=1}^{\infty}\left[\left(1-\frac{z}{an+b}\right)\exp(z/an)\right], \tag{B 7}$$

with E the Euler constant, together with the asymptotic formula

$$\Gamma(Az+B) \sim (2\pi)^{\frac{1}{2}}\exp(-Az)(Az)^{Az+B-\frac{1}{2}}, \tag{B 8}$$

finally yields that

$$\prod_{n=1}^{\infty}\left(1-\frac{z}{a_n}\right)\exp(z/a_n) \sim \exp\left[-\left(-\frac{z}{a}+\frac{b}{a}+\frac{1}{2}\right)\ln\left(-\frac{z}{a}\right) - \frac{z(1-E)}{a}+z\sum_{n=1}^{\infty}\left(\frac{1}{a_n}-\frac{1}{an}\right)\right]. \tag{B 9}$$

Now, given that

$$k_n^- \sim -\mathrm{i}\frac{\pi n}{\beta s}-\frac{M^2\Omega}{\beta^2}, \tag{B 10a}$$

$$\sigma_n^- \sim \left(\frac{2\pi d-2\pi \mathrm{i}s\beta}{d^2+s^2\beta^2}\right)n+\frac{-(\mathrm{i}sdM^2\Omega/\beta)+\mathrm{i}s\beta\sigma-M^2\Omega s^2-\mathrm{d}\sigma}{d^2+s^2\beta^2} \tag{B 10b}$$

and

$$\sigma_{-n}^- \sim \left(\frac{-2\pi d-2\pi \mathrm{i}s\beta}{d^2+s^2\beta^2}\right)n+\frac{(\mathrm{i}sdM^2\Omega/\beta)-\mathrm{i}s\beta\sigma-M^2\Omega s^2-\mathrm{d}\sigma}{d^2+s^2\beta^2} \tag{B 10c}$$

as $n \to +\infty$, substitution of (B 9) and (B 10a–c) into (B 4) demonstrates that the necessary choice of $\chi(k)$ is

$$\chi(k) = (\mathrm{i}d\theta/\pi-\tfrac{1}{2}\mathrm{i}d-(\mathrm{i}s\beta/\pi)\ln\tfrac{1}{2}\operatorname{cosec}\theta)k, \tag{B 11}$$

where $\tan\theta = s\beta/d$. The analysis also reveals that, given this choice of χ,

$$\mathscr{K}^+(k) \sim k^{\frac{1}{2}}$$

as $k \to \infty$ in R^+.

The equivalent expression for $\mathscr{K}^-(k)$ can easily be derived from $\mathscr{K}/\mathscr{K}^+$, and it can be shown that $\mathscr{K}^-(k) \sim k^{-\frac{1}{2}}$ as $k \to \infty$ in R^-.

REFERENCES

ABRAMOWITZ, M. & STEGUN, I. A. 1968 *Handbook of Mathematical Functions*. Dover.

ADAMCZYK, J. J. & GOLDSTEIN, M. E. 1978 Unsteady flow in a supersonic cascade with subsonic leading-edge locus. *AIAA J.* **16** 1248–1254.

CARGILL, A. M. 1988 On high frequency cascade/gust interaction. *Rolls-Royce Rep.* TSG 0419.

CARLSON, J. F. & HEINS, A. E. 1946 The reflection of electromagnetic waves by an infinite set of plates, I. *Q. Appl. Maths.* **4**, 313–329.

CRIGHTON, D. G. 1971 Acoustic beaming and reflexion from wave-bearing surfaces. *J. Fluid Mech.* **47**, 625–638.

CRIGHTON, D. G. 1985 The Kutta condition in unsteady flow. *Ann. Rev. Fluid Mech.* **17**, 411–445.

GOLDSTEIN, M. E. 1976 *Aeroacoustics*. McGraw-Hill.

HEINS, A. E. 1950 The reflection of electromagnetic waves by an infinite set of plates, III. *Q. Appl. Maths.* **8**, 281–291.

HEINS, A. E. & CARLSON, J. F. 1947 The reflection of electromagnetic waves by an infinite set of plates, II. *Q. Appl. Maths.* **5**, 82–88.

JONES, D. S. 1986 *Acoustic and Electromagnetic Waves*. Oxford University Press.

KAJI, S. & OKAZAKI, T. 1970*a* Propagation of sound waves through a blade row I. Analysis based on the semi-actuator disk theory. *J. Sound Vib.* **11**, 339–353.

KAJI, S. & OKAZAKI, T. 1970*b* Propagation of sound waves through a blade row II. Analysis based on the acceleration potential method. *J. Sound Vib.* **11**, 355–375.

KOCH, W. 1971 On the transmission of sound waves through a blade row. *J. Sound Vib.* **18**, 111–128.

KOCH, W. 1983 Resonant acoustic frequencies of flat plate cascades. *J. Sound Vib.* **88**, 233–242.

KOITER, W. T. 1954 Approximate solution of Wiener–Hopf type integral equations with applications, I–III. *Koninkl. Ned. Akad. Wetenschap. Proc.* B **57**, 558–579.

LANDAHL, M. 1989 *Unsteady Transonic Flow*. Cambridge University Press.

LIGHTHILL, M. J. 1952 On sound generated aerodynamically. I. General theory. *Proc. R. Soc. Lond.* A **211**, 564–587.

LIGHTHILL, M. J. 1954 On sound generated aerodynamically. II. Turbulence as a source of sound. *Proc. R. Soc. Lond.* A **222**, 1–32.

LIGHTHILL, M. J. 1958 *An Introduction to Fourier Analysis and Generalised Functions*. Cambridge University Press.

MANI, R. & HORVAY, G. 1970 Sound transmission through blade rows. *J. Sound Vib.* **12**, 59–83.

MEISTER, E. 1962*a* Zum Dirichlet-Problem der Helmholtzschen Schwingungsgleichung fur ein gestaffeltes Streckengitter. *Arch. Rat. Mech. Anal.* **10**, 67–100.

MEISTER, E. 1962*b* Zum Neumann-Problem der Helmholtzschen Schwingungsgleichung fur ein gestaffeltes Streckengitter. *Arch. Rat. Mech. Anal.* **10**, 127–148.

NOBLE, B. 1958 *Methods based on the Wiener–Hopf technique*. Pergamon.

PARRY, A. B. & CRIGHTON, D. G. 1989 Prediction of counter-rotation propeller noise. *AIAA Paper* 89–1141.

SCHWARZSCHILD, K. 1901 Die beugung und polarisation des lichts durch einen spalt – I. *Math. Ann.* **55**, 177–247.

VERDON, J. M. & HALL, K. C. 1990 Development of a linearised unsteady aerodynamic analysis for cascade gust response predictions. *NASA Rep.* CR-4308.

WHITEHEAD, D. S. 1970 Vibration and sound generation in a cascade of flat plates in subsonic flow. *University of Cambridge Department of Engineering Rep. CUED/A-Turbo/Tr* 15.